Journal of Petroleum Science and Engineering 207 (2021) 109165

Contents lists available at ScienceDirect

Journal of Petroleum Science and Engineering

journal homepage: www.elsevier.com/locate/petrol

Ensemble-based constrained optimization using an exterior penalty method

Micheal B. Oguntola [a,b,*], Rolf J. Lorentzen [b]

[a] University of Stavanger, 4036, Stavanger, Norway
[b] NORCE-Norwegian Research Center AS, 5838, Bergen, Norway

ARTICLE INFO

Keywords:
Ensemble-based optimization
Stochastic gradient
Constrained optimization
Penalty method
Line search method
Production optimization
Lagrange method

ABSTRACT

In science and engineering, non-linear constrained optimization has been a useful mathematical technique for many practical applications. Of interest to us is its applicability in the modeling and prediction of hydrocarbon reservoir production. In this paper, a new efficient, robust, and accurate optimal solution strategy based on the exterior penalty function (EPF) method and the adaptive ensemble-based optimization (EnOpt) approach (with backtracking line-search technique) for non-linear constrained optimization problems is presented. The purpose of this work is to provide a better user-friendly strategy which mitigates the problem often faced with the current constraints handling technique utilized when using the EnOpt method to solve constrained problems of water or EOR flooding. This study notes that the problem contributes to uncertainties in the gradient computation of the objective function and hence leads to the poor convergence rate of the standard EnOpt method. In this work, we used the EPF method to transform a given constrained optimization problem to a sequence of unconstrained subproblems and then sequentially solve the subproblems by unconstrained EnOpt procedure until convergence to the solution of the original problem. To demonstrate the advantage of the proposed methodology, we used it to solve analytical 2D bound constrained Rosenbrock's problem and a practical high dimensional bound constrained water flooding optimization problem associated with a 2D 5Spot field and a 3D Reek reservoir field. The numerical results are compared with EnOpt using classical Lagrangian approach, as well as the traditional EnOpt. Our findings showed that the proposed solution method has a fast convergence rate and is more accurate and robust.

1. Introduction

In reservoir production optimization, finding an injection/ production strategy (with high precision) for a particular oil recovery method that is economical at the expense of little or no negative environmental impact for a given reservoir type can be problematic. One reason for this problem is based on how the uncertain geological parameters in the reservoir of interest are quantified and utilized in the solution method for the reservoir optimization problem. Having a good quantification of the uncertain parameters using production history in reservoir studies has been the major contribution of closed-loop reservoir management (Aanonsen et al., 2009; Jansen et al., 2009; Jung et al., 2018; Zhang et al., 2019; Mirzaei-Paiaman et al., 2021). Several solution methods for the non-linear constrained optimization problems (Nocedal and Wright, 2006), usually encountered in hydrocarbon reservoir fields have been proposed and used extensively for different applications (see e.g., Sarma et al. (2005, 2006), Jansen (2011), Li and Reynolds (2011), Zhou et al. (2013), Xu et al. (2018) and Zhao et al. (2020)). For instance, of interest to us is the ensemble-based optimization (EnOpt) method, a popular and robust stochastic optimization technique, first introduced in Lorentzen et al. (2006), and further developed into its current form in Chen et al. (2009, 2010) and Fonseca et al. (2014). In EnOpt, the uncertainty descriptions in the reservoir are taken into account. However, the current constraint handling technique often utilized in the EnOpt method (see Chen et al. (2009)) poses uncertainty in the optimization result, which thus reduces its accuracy. In this study, we presented a more accurate means to deal with the constraints of the optimization problem in EnOpt by using the penalty function (PF) method (Nocedal and Wright, 2006; Rao, 2019). We demonstrate the convergence and added advantage (in terms of accuracy compared to the standard method) of the proposed coupling (of the PF method with EnOpt) using analytical and practical examples.

In constrained optimization problems, usually, one sorts to find the best feasible solution (out of a pull of solutions) called the optimal solution for the control variables that gives the extremum of a given objective function subject to a set of equality and/or inequality constraints. Here, feasibility implies that the underlying constraints are satisfied. In practice, the design of the control variables could take different forms. For instance, in reservoir optimization problems, the

* Corresponding author at: University of Stavanger, 4036, Stavanger, Norway.
E-mail address: micheal.b.oguntola@uis.no (M.B. Oguntola).

https://doi.org/10.1016/j.petrol.2021.109165
Received 17 February 2021; Received in revised form 22 June 2021; Accepted 25 June 2021
Available online 29 June 2021

control variables could include the number of well-type (producer or injector) to be sequentially drilled, their drilling order and location, the operational controls (such as the well-rates or bottom hole pressures over the production period), etc. Whence, the total number of control variables to be optimized is often of the order 100 and above. The objective function is usually some reservoir performance measures (such as net present value (NPV), oil recovery factor (ORF), etc.) defined on the given set of control variables. Several methods (with advantages and disadvantages Islam et al., 2020) have been established to find the optimal solutions to the optimization problems. They are majorly categorized as gradient-based and derivative-free techniques (Jesmani et al., 2020). Each of the techniques moves in the design solution space in a special pattern in search of the optimal solution. The gradient-based method mainly utilize (either analytically or by approximation) the derivatives of the objective function with respect to the control variables to control the search pattern while the derivative-free methods mostly use the objective function values in a stochastic way at each optimization iteration. The derivative-free methods are known to be computationally very efficient for low dimensional problems but struggle to converge once the dimension of problem is high (Arouri and Sayyafzadeh, 2020) (for a detailed review of the derivative-free methods, we refer interested readers to the work of Chen et al. (2020) and Semnani et al. (2021). Because of the large size of unknown variables often encounter in reservoir optimization problems, the gradient-based methods are more suitable to use.

Several gradient-based methods have been devised and utilized to solve different optimization problems such as well placement and control problems (Hutahaean et al., 2019; Liu et al., 2019; Sun et al., 2019; Epelle and Gerogiorgis, 2020). In terms of efficiency and accuracy, the adjoint method is ranked number one on the list of gradient-based methods because of its efficient and accurate gradient computation. However, for practical optimization applications such as the one in the management of subsurface hydrocarbon reservoirs, the adjoint method becomes very difficult to implement because (1) the adjoint-based gradient calculation with respect to the control variables is complicated and cannot be directly reused for different problems; (2) it requires user access to the reservoir simulator (Sarma et al., 2005, 2006; Jansen, 2011). To avoid the problem (1) faced with the adjoint method in well placement optimization, indirect approaches were developed (see, for e.g. Sarma et al. (2008) and Zandvliet et al. (2008)). However, problem (2) is inevitable. For these reasons, viable alternative solution methods that do not rely the adjoint method of gradient calculation are developed. The simplest one is the finite difference gradient approximation (FDGA) method which uses finite difference scheme to approximate each component of the gradient. In this case, at each iteration, the approximate gradient computation requires $2N_u$ function evaluations, where N_u is the size of the unknown variables to be optimized. Therefore, for high-dimensional problems, the FDGA method becomes computationally very expensive to use (Zhou et al., 2013; Jesmani et al., 2020). Other approximate gradient-based solution methods that are more efficient than the FDGA have been proposed in the literature. The most popular ones for reservoir optimization are the simultaneous perturbation stochastic approximation (SPSA) (Spall, 1998; Spall et al., 2006; Foroud et al., 2018), modified SPSA based on finite difference method (SPSA-FDG) (Zhou et al., 2013), the stochastic simplex approximation gradient (StoSAG) method Fonseca et al. (2017), and the ensemble-based optimization (EnOpt) method (Chen et al., 2010). These solution methods approximate the gradient of the objective function by simultaneously perturbing all the unknown variables at the same time, unlike the FDGA method where one variable is perturbed at a time. Theoretically, it has been proven by Do and Reynolds (2013) using the steepest descent scheme that a small difference in gradient computation exists between StoSAG, EnOpt, and SPSA (as well as its variants such as Gaussian-SPSA) methods. These methods have gained popularity recently due to their ability to incorporate uncertainty represented by multiple realizations of the reservoir model in their approximate gradient computation (Hutahaean et al., 2019; Jesmani et al., 2020).

The standard EnOpt is an iterative method, formulated based on a first-order inexact line search (with a simple backtracking technique Nocedal and Wright, 2006) steepest ascent optimization method (Snyman and Wilke, 2018). In this case, the approximate gradient of the objective function (in the line search direction) at each iterate is computed using a stochastic process. At each iteration, an ensemble of control vectors is sampled from a multivariate Gaussian distribution with a known mean (same as the current iterate) and a user-defined covariance matrix to compute the sample cross-covariance of the objective function and control variables. Using suitable assumptions, it is not hard to show that the sample cross-covariance is approximately the (regularized) gradient of the objective function (Chen et al., 2010; Do and Reynolds, 2013). Therefore, pressing issues with EnOpt will mainly be on the quantities (or inputs) that can impact the accuracy of the estimated gradient needed for a considerable increase in the objective function value at subsequent optimization iterations. In other words, uncertainty can be introduced by some quantities in the line search direction utilized in the EnOpt iterative method. Inappropriate choice of some of these quantities have proven to affect the convergence rate of the method. Sometimes, this could translate to the need for a higher number of iterations for convergence. To mention a few, quantities such as the ensemble size, sampling strategies, and distribution covariance matrix (or the perturbation size), etc., have been extensively studied in the literature. For instance, Fonseca et al. (2015) investigated the impact of ensemble size on the quality of the approximate EnOpt gradients (by comparing it with the exact adjoint gradient) for the Rosenbrock optimization problems and for a hydrocarbon reservoir. In their study, they provided a more computationally efficient and modified version of EnOpt using hypothesis testing. In other studies by Fonseca et al. (2014) and Stordal et al. (2016), they found that by systematically updating the perturbation size (through a method called covariance matrix adaptation (CMA)) at each optimization iteration would effectively improve the quality of the approximate gradient. Ramaswamy et al. (2020) evaluated the impact of different sampling strategies on the performance of the approximate EnOpt gradient for high-dimensional analytical and robust optimization problems. Their findings suggested the sampling design to consider in general for gradient approximation schemes in supersaturated cases, i.e., where the number of perturbation vector is less than the optimization unknowns. Zhang et al. (2018a,b) considered a slightly different iterative scheme, the trust region method with the conjugate gradient method rather than the line search method often utilized in EnOpt and demonstrated a fast convergence rate with applications on simple toy and synthetic reservoir problems.

Over recent years, the EnOpt method has received a lot of treatments towards improving its efficiency and accuracy, as mentioned above. However, in practice, we found that constrained optimization problems solved using the EnOpt technique were dealt with in an unconstrained manner. In reservoir optimization problems, there is usually a set of bound constraints imposed on the designed control variables. A common way to deal with this is to systematically discard or truncate values of control variables that do not satisfy the constraints, which leads to inaccurate gradient directions. An alternative is to use some transformation (see e.g., Chen et al. (2009) and Do and Reynolds (2013)) to enforce the constraints on the respective control variables. A transformation is not always advisable, especially for problems with complex non-linear constraints. Consequently, both truncation or transformation of control variables can contribute to uncertainties in the computation of the approximate gradient and hence lead to poor convergence to a desired local optimum. For this reason, we introduce a better and user-friendly approach, the PF method, to deal with constraints when using the EnOpt method to solve constrained optimization problems.

The PF method belongs to an important class of solution methods for constrained optimization problems. It transforms a given constrained

problem into a sequence of unconstrained subproblems. See Nocedal and Wright (2006), Sun and Yuan (2006), Deb (2012) and Rao (2019) for a concrete theoretical overview of the PF method. In each subproblem, there exists a penalty function constructed by adding a penalty term (which is the constraint violation multiplied by a penalty parameter) to the objective function. Usually, the penalty term takes different forms depending on the type of constraint (equality or inequality). So, if an estimate of a control variable violates a given constraint, the objective function is penalized by an amount measured by the penalty term. More efficiently and robustly, the PF method works by sequentially solving each subproblem using a suitable unconstrained optimization procedure. In this case, the optimum found in one subproblem is utilized as the initial guess for the next unconstrained subproblem. In the subsequent subproblems, the solution improves gradually and eventually converges to the desired optimum of the original constrained optimization problem. However, we noted that the choice (in terms of initialization and subsequent adaptation) of the penalty parameter in the penalty term is very crucial to the convergence rate. Our study adopts the ideas in Nocedal and Wright (2006) and Rao (2019) for the adaption of the penalty parameter and hence the structure of the penalty term.

Over time, the PF method has evolved and its approach has been utilized to solve constrained problems in different areas of science and engineering. For instance, Zhang et al. (2016) used a variant of the PF method, the augmented Lagrangian method, and a stochastic gradient finite difference (SGFD) approach (Yan and Reynolds, 2014) to solve constrained oil reservoir optimization problem. They showed that the combined strategies give accurate results based on their comparison of SGFD and Gaussian distribution Simultaneous Perturbation Stochastic Approximation (G-SPSA) on simple high dimensional constrained analytical problem. However, the said SGFD is not very efficient compared to the EnOpt method because of the higher number of function evaluations and required storage associated with SGFD, especially for complex high dimensional constrained problems.

In this paper we present an efficient, accurate, and robust extension of EnOpt, to solve non-linear constrained optimization problems often encounter in science and engineering. We employ the exterior penalty function method with bracket operator (for inequality constraints) penalty term (Deb, 2012) to transform the original constrained optimization problems into a sequence of unconstrained subproblems and then utilize the adaptive EnOpt method as the unconstrained optimization procedure. For simplicity, we refer to the combined strategies as the EPF-EnOpt method. Our choice of the exterior PF is to allow for the flexibility of initialization for the unconstrained optimization procedure. We provide proof of convergence of the EPF method using suitable assumptions. Further, we demonstrate the use of the methodology with a challenging constrained analytical problem and practical constrained 2D 5-spot and 3D Reek oil reservoir problems and compare results with the standard EnOpt approach. In addition, we compare the EPF-EnOpt results with the classical Lagrangian constraint handling technique (similar to the formulation in Deb (2012) and Lu et al. (2017)) coupled with the standard EnOpt for the 3D Reek field to further illustrate the efficiency and accuracy of our proposed method. The Lagrange multiplier is estimated using a scheme similar to the one in Snyman and Wilke (2018). The rest of the paper is as follows; Section 2 discusses the mathematical model of constrained optimization problems. Section 3 looks at the theory of the exterior PF formulation for general constrained optimization problems and the derivation of the adaptive EnOpt procedures. Section 4 builds on previous sections to formulate the EPF-EnOpt algorithm and discuss its convergence, and finally, Sections 5 and 6 present applications (with relevant discussion) and conclusion, respectively.

2. Constrained optimization problem and techniques

The mathematical model of constrained optimization is useful for many applications in science and engineering. For instance, in hydrocarbon reservoir management, resources such as the injecting and producing facilities are limited in capacities. Therefore, the optimization of the objective function, usually a given reservoir performance index (such as the oil recovery factor or the net present value (NPV), etc.) is necessarily subject to a well-defined set of constraints on the designed control variables (such as the water rate of each injecting well at each control time step, etc.). This is usually referred to as an optimal control problem during reservoir development, and the goal of this problem is to find the best (optimal) strategy of control variables for maximum profit.

In this section, we present a general constrained optimization (maximization) problem, often encountered in science and engineering. Let $\mathbf{u} \in \mathbb{R}^{N_u}$ be the vector of designed control variables (optimization unknowns) i.e, $\mathbf{u} = [u_1, u_2, \dots, u_{N_u}]^{\mathsf{T}}$ (T means transpose). Again, the form of $\mathbf{u}$ can differ for different problems. In reservoir optimization problems, the components of $\mathbf{u}$ can represent the wells (injectors or producers) target rates or bottom hole pressures in a specific control time step during water flooding. The general N_u-dimensional constrained optimization problem is to find the optimum /best $\mathbf{u} \in \mathbb{R}^{N_u}$ that

$$\underset{\mathbf{u}\in\mathbb{R}^{N_u}}{\text{maximize}} \quad J(\mathbf{u}) \tag{1}$$

$$\text{subject to:} \quad g_i(\mathbf{u}) \geq 0, \quad \forall i \in \mathrm{I} \tag{2}$$

$$h_j(\mathbf{u}) = 0, \quad \forall j \in \mathrm{E}, \tag{3}$$

where J is the objective function (from $\mathbb{R}^{N_u}$ into $\mathbb{R}$), g_i and h_j are the underlying constraint functions (from $\mathbb{R}^{N_u}$ into $\mathbb{R}$ respectively), I and E are the indexing sets for the inequality and equality constraints respectively. The optimization problem stated in Equations (1) - (3) becomes unconstrained should $\mathrm{I} \cup \mathrm{E} = \emptyset$. Since,

$$\max_{\mathbf{u}\in\mathbb{R}^{N_u}} J(\mathbf{u}) = -\min_{\mathbf{u}\in\mathbb{R}^{N_u}} (-J(\mathbf{u})), \tag{4}$$

without the loss of generality, the maximization problem (1) - (3) can be considered as a minimization problem by replacing (1) with (4). Therefore, the focus of this study is on constrained minimization problems of the type:

$$\min_{\mathbf{u}\in\mathbb{R}^{N_u}} f(\mathbf{u}) \tag{5}$$

$$\text{subject to:} \quad g_i(\mathbf{u}) \geq 0, \quad \forall i \in \mathrm{I} \tag{6}$$

$$h_j(\mathbf{u}) = 0, \quad \forall j \in \mathrm{E}, \tag{7}$$

where f is a continuous objective function. The structure of the constraints in Eqs. (6)–(7) varies from one problem to another. In reservoir optimization problems constraints are often given as linear inequality constraints. The simplest type are bound constraints where each inequality only depends on a single control variable. In this case, suppose that u_i^{low} and u_i^{upp} are the lower and upper bounds respectively for each control variable u_i, the bound constraints are given as:

$$u_i^{\text{low}} \leq u_i \leq u_i^{\text{upp}}, \qquad \forall i \in 1, 2, \dots, N_u. \tag{8}$$

Constraint types called the “output constraints” in the petroleum industry are also very commonly utilized during petroleum production. These are non-linear constraints that represent operational limits and they are usually evaluated using the reservoir simulator. A typical example is pressure limits for injectors or producers in a model where the wells are operated using flow rate targets (given by the control variables). Our primary goal with this paper is handling of bound constraints, but, it is not limited to this alone as the exterior PF methodology can be used for complicated constraints (like the output constraints). However, as a common practice, one could let the reservoir simulator handle the output constraints. Next, we explain two traditional ways in the literature to handle the bound constraints, and then we continue with the methodology using the exterior PF.

2.1. Bound constraints transformation

Suppose that Eq. (8) is the only set of constraints impose on the control variables in the optimization problem (5)–(7). A given optimal solution method like the EnOpt method finds an approximate solution that solves the optimization problem until convergences. At each optimization iteration, to ensure that each solution obtained is feasible, i.e., the underlying constraints are satisfied, either of the following two procedures is useful.

1. Linear transformation with truncation.
   For each $i \in \{1, 2, \dots, N_u\}$, a bijective linear function is defined to transform the domain of the control variable u_i into the closed interval $[0, 1]$. That is

$$T_i : [u_i^{\text{low}}, u_i^{\text{upp}}] \longrightarrow [0, 1], \tag{9}$$
$$u_i \longmapsto T_i(u_i) := \hat{u}_i = \frac{u_i - u_i^{\text{low}}}{u_i^{\text{upp}} - u_i^{\text{low}}}, \quad u_i^{\text{upp}} \neq u_i^{\text{low}}$$

   (this transformation follows from the result of a simple algebraic rearrangement of the inequalities in Eqs. (8), and then divide through by $u_i^{\text{upp}} - u_i^{\text{low}}$), where $\hat{u}_i$ is the transformed control variable u_i. In this case, the optimization process is carried out in the interval $[0, 1]$. Because the linear function (9) is bijective, its inverse exist. Thus, any value of $\hat{u}_i$ found can easily be transformed into its equivalent value in the domain $[u_i^{\text{low}}, u_i^{\text{upp}}]$ by using;

$$u_i = (u_i^{\text{upp}} - u_i^{\text{low}})\hat{u}_i + u_i^{\text{low}}. \tag{10}$$

   Here, any value of $\hat{u}_i$ that falls outside the closed interval $[0, 1]$ is systematically approximated (or truncated) as follows;

$$\hat{u}_i = \begin{cases} 1, & \text{if } \hat{u}_i > 1 \\ 0, & \text{if } \hat{u}_i < 0. \end{cases} \tag{11}$$

   Vital estimates of control variables for accurate gradient directions can easily be lost using this truncation. As a consequence, this can affect the convergence rate of the solution method.
2. Logarithmic transformation.
   Here, for each u_i, $i \in \{1, 2, \dots, N_u\}$, a logarithmic (log) function is used to transform the domain (excluding the boundary points) of u_i to the entire set of real numbers i.e, $\mathbb{R} = (-\infty, +\infty)$. The transformation is defined by:

$$L_i : (u_i^{\text{low}}, u_i^{\text{upp}}) \longrightarrow (-\infty, +\infty) \tag{12}$$
$$u_i \longmapsto L_i(u_i) := \hat{u}_i = \log_e\left(\frac{u_i - u_i^{\text{low}}}{u_i^{\text{upp}} - u_i}\right).$$

   In this case, the optimization procedure occurs in the transformed domain, $(-\infty, +\infty)$. Therefore, since $[0, 1] \subset (-\infty, +\infty)$, the transformed optimization unknown, $\hat{u}_i$ can now fluctuate or vary in a set of points larger than the optimization domain obtained from the linear transformation. Similarly, L_i is a well-defined bijective function and hence its inverse can be computed as;

$$u_i = \frac{u_i^{\text{upp}} \exp(\hat{u}_i) + u_i^{\text{low}}}{\exp(\hat{u}_i) + 1}. \tag{13}$$

   Using the log transformation helps to reduce the possibility of truncation often encounter with the linear transformation. However, if the initial solution guess is close to the boundary, it is difficult to find a suitable gradient direction for improvements. In addition, problems in which the optimal solution of one or more control variables lie on the boundary of the solution domain can be hard to solve. It is because of the following simple observation (from Eq. (12));

$$\hat{u}_i = \begin{cases} +\infty, & \text{if } u_i = u_i^{\text{low}} \\ -\infty, & \text{if } u_i = u_i^{\text{upp}} \end{cases} \tag{14}$$

   whereas, neither $u_i^{\text{low}}, u_i^{\text{upp}} \in (u_i^{\text{low}}, u_i^{\text{upp}})$ nor $-\infty, +\infty \in (-\infty, +\infty)$.

Application of any of the described procedures above transforms the given constrained optimization problem (with only bound constraints) in Eqs. (5)–(7) to an unconstrained optimization problem. The resulting unconstrained optimization problem is then solved by suitable unconstrained minimization methods (like the ones considered in Li and Reynolds (2011), Do and Reynolds (2013), Zhao et al. (2013) and Zhou et al. (2013), etc.) and thus leading to the solution of the initial/original constrained optimization problem (5)–(7). This has been a common practice, especially in the petroleum industries.

In addition to the shortcomings mentioned above, the procedures of handling bound constraints cannot easily be extended to more complicated (possibly non-linear) equality or inequality constraints. Next in this study, we present a more accurate method to solve a general constrained minimization problems.

3. Exterior PF formulation

Suppose that a given constrained optimization problem is in the form of Eqs. (5)–(7). Let $\mathcal{D} \subset \mathbb{R}^{N_u}$ be the domain of feasible solutions. Hence, $\mathbb{R}^{N_u} \backslash \mathcal{D}$ is the set of infeasible points. To solve the problem, first, we transform it into a sequence of unconstrained subproblems, $\{P_k\}_{k=1}^{\infty}$ using the exterior quadratic PF method. In each subproblem, P_k, $k = 1, 2, \dots$, is a penalty function defined as follows;

$$P_k : \mathbb{R}^{N_u} \times (0, +\infty) \longrightarrow \mathbb{R} \tag{15}$$
$$(\mathbf{u}, r_k) \longmapsto P_k(\mathbf{u}, r_k) = f(\mathbf{u}) + r_k \underbrace{\left(\sum_{i \in \mathrm{I}} (\min\{g_i(\mathbf{u}), 0\})^2 + \sum_{j \in \mathrm{E}} |h_j(\mathbf{u})|^2\right)}_{Q(\mathbf{u})}$$

$\big($we set, $P_k := P_k(\mathbf{u}, r_k)\big)$, where $\{r_k\}_{k=1}^{\infty}$ is an increasing sequence of positive penalty parameters (which control the iteration of P_k) well-defined such that

$$\lim_{k \to +\infty} r_k = +\infty. \tag{16}$$

For convenience, we consider a simple sequence of penalty parameters given by the relation

$$r_{k+1} = c r_k, \quad k = 1, 2, \dots, \tag{17}$$

where $c \geq 1$ and the first term, $r_1 > 0$ are carefully selected constants. Different values of r_1 can mean different number of subproblems to solve before convergence. Cases of subproblems with exact penalty functions have been treated extensively (we refer readers to Han and Mangasarian (1979) and Nocedal and Wright (2006) for more information on the impact of the different selection criteria for r_1). For each $i \in \mathrm{I}$, we define the bracket operator on $g_i(\mathbf{u})$ as

$$\min\{g_i(\mathbf{u}), 0\} = \begin{cases} g_i(\mathbf{u}), & \text{if } g_i(\mathbf{u}) < 0 \\ & \text{(i.e. } \mathbf{u} \in \mathbb{R}^{N_u} \backslash \mathcal{D} \text{ (constraint is violated))} \\ 0, & \text{if } g_i(\mathbf{u}) \geq 0 \\ & \text{(i.e. } \mathbf{u} \in \mathcal{D} \text{ (constraint is satisfied))} \end{cases} \tag{18}$$

and for each $j \in \mathrm{E}$,

$$|h_j(\mathbf{u})| = \begin{cases} -h_j(\mathbf{u}), & \text{if } h_j(\mathbf{u}) < 0 \\ & \text{(i.e. } \mathbf{u} \in \mathbb{R}^{N_u} \backslash \mathcal{D} \text{ (constraint is violated))} \\ 0, & \text{if } h_j(\mathbf{u}) = 0 \\ & \text{(i.e. } \mathbf{u} \in \mathcal{D} \text{ (constraint is satisfied))} \\ h_j(\mathbf{u}), & \text{if } h_j(\mathbf{u}) > 0 \\ & \text{(i.e. } \mathbf{u} \in \mathbb{R}^{N_u} \backslash \mathcal{D} \text{ (constraint is violated)).} \end{cases} \tag{19}$$

Since h_j is a real-valued function, then $|h_j|^2 = h_j^2$, and hence Eq. (19) can be neglected. However, in a situation where an l_1-penalty function

definition (Nocedal and Wright, 2006) is used in Eq. (15) or a complex-valued function h_j is considered, then (19) is retained. In Eq. (15), Q is called the exterior penalty term defined based on the given constraints (6)–(7). When a given estimate of the control vector $\mathbf{u}$ is infeasible to a given constraint, it means a violation of the constraint by the estimate. For such a violation, we penalize the objective function by an amount measured by Q. Therefore, using Eqs. (18) and (19), it is not hard to see that for a feasible solution, Q is zero and for an infeasible solution, Q is positive with an amount proportional to the square of the value given by Eq. (18) (for inequality constraint) and/ or Eq. (19) (for equality constraints). So, in general:

$$Q(\mathbf{u}) \geq 0, \quad \forall \mathbf{u} \in \mathbb{R}^{N_u}. \tag{20}$$

Next, we sequentially (with successively increasing r_k values) solve the subproblem

$$\min_{\mathbf{u}\in\mathbb{R}^{N_u}} P_k(\mathbf{u}, r_k), \quad \forall k = 1, 2, \dots, \tag{21}$$

where P_k is defined by Eq. (15) (and we will often replace the pair $(\mathbf{u}, r_k)$ by $\mathbf{u}(r_k)$ in the rest of this section) and r_k is defined by Eq. (17). This is an unconstrained optimization problem. Note that P_k is non-differentiable at the points $\mathbf{u}$ that lie on the border between the feasible and the infeasible domains (because of Eqs. (18) and (19)), that is its gradient does not exist at the said points. Therefore, unconstrained numerical solution methods based on analytic gradient computation is not suitable. The bundle methods solve non-differentiable optimization problems more effectively and are reliable (Bagirov et al., 2014). However, for an extensive application, we instead utilize the EnOpt method, which does not rely directly on analytic gradient. For any $r_k, k = 1, 2, \dots$, the EnOpt method finds an approximate minimum point of P_k, denoted by $\mathbf{u}_k^* := \mathbf{u}^*(r_k)$. Usually, P_k possesses a minimum as a function of $\mathbf{u}$ in the infeasible region, especially when its initial guess, $\mathbf{u}_{k-1}$ is an infeasible point. The sequence of unconstrained minima denoted by $\mathbf{u}_k^*, k = 1, 2, \dots$ converges to the desired minimizer of the original constrained optimization problem (5)–(7) as $k \to +\infty$. Therefore, $\mathbf{u}_k^*$ approaches the feasible domain gradually, and eventually lies in the feasible region (equivalently, $|Q(\mathbf{u}_k^*)| \to 0$) as $r_k \to +\infty$, with $k \to +\infty$.

The EnOpt method for solving the unconstrained optimization problem of the type presented in Eq. (21) is next described.

3.1. EnOpt procedures

We consider the problem (21) for any fixed penalty parameter, r_k. The EnOpt is an iterative optimal solution method in which the user starts by selecting an initial control vector $\mathbf{u}_1$ according to some rules, and then proceed to find the best approximation to the optimum solution $\mathbf{u}$, that minimizes $P_k(\mathbf{u}, r_k)$ using a preconditioned gradient descent method given by

$$\mathbf{u}_{l+1} = \mathbf{u}_l - \frac{1}{\beta_l} \frac{\mathbf{C}_\mathbf{u}^l \mathbf{G}_l^\top}{\|\mathbf{C}_\mathbf{u}^l \mathbf{G}_l^\top\|_2}, \quad \forall l = 1, 2, \dots, \tag{22}$$

until convergence, where l is the iteration index; $\mathbf{G}_l$ is the sensitivity (an approximate gradient) of $P_k(\mathbf{u}, r_k)$ with respect to the control variables $u_i, i = 1, 2, \dots, N_u$, also called the search direction at the lth iteration; β_l is the tuning parameter for iteration step size. It is used to ensure a sufficient descend along the search direction. Here, we employ the backtracking line search method (Nocedal and Wright, 2006) to compute (and update when necessary) β_l at each iteration (see Algorithm 1). $\mathbf{C}_\mathbf{u}^l$ denotes a real symmetric positive definite matrix defined as the covariance matrix of control variables at the lth iteration; $\|.\|_2$ is the l_2- norm. In hydrocarbon reservoir management, it is not very common to have controls (like water rate and oil rate) at different wells (injector and producer) to correlate. However, the water rate (for example) of a particular injection well can be correlated in time throughout the production period in a water flooding scenario. Because of this, in Eq. (22), $\mathbf{C}_\mathbf{u}^l$ is defined to avoid inappropriate dependence among control variables. It also ensures possible smoothness, correlation, and long-term fluctuations in the control variables of the same kind (Do and Reynolds, 2013).

We initialize the covariance matrix, $\mathbf{C}_\mathbf{u}^l$ differently at the start of iteration, $l = 1$ for the different optimization problems considered in this study. For analytical problem (like the 2D Rosenbrock problem Snyman and Wilke, 2018) where the N_u-unknowns are distinct and do not need to be correlated over time, we used a $N_u \times N_u-$ diagonal matrix where the variances of unknown variables are the diagonal elements. Suppose that $\sigma_i^2, i = 1, 2, 3, \dots, N_u$ is the variance of the unknown control variable $u_i, i = 1, 2, \dots, N_u$ respectively. The initial covariance matrix is taken as

$$\mathbf{C}_\mathbf{u}^1 = \begin{pmatrix} \sigma_1^2 & 0 & 0 & \dots & 0 \\ 0 & \sigma_2^2 & 0 & \dots & 0 \\ \cdot & & & & \\ \cdot & & & & \\ \cdot & & & & \\ 0 & 0 & 0 & \dots & \sigma_{N_u}^2 \end{pmatrix}. \tag{23}$$

For the water flooding reservoir optimization problem considered in this study, we initialize the covariance matrix, $\mathbf{C}_\mathbf{u}^l$ using a stationary AR(1) model (similar to the one in Oguntola and Lorentzen (2020)) to simulate the correlation of control variables at individual well and assume control variables at different wells are not correlated. To achieve this scenario, we used the following covariance function:

$$\mathrm{Cov}(u^m[t], u^m[t+h]) = \sigma_m^2 \rho^h \left(\frac{1}{1-\rho^2}\right), \quad \forall\ h \in [0, N_t - t], \tag{24}$$

where $u^m[t]$ is the control variable of well $m = 1, 2, \dots, N_{\text{well}}$ at the control time step t, N_{well} is the total number of wells, σ_m^2 is the variance for the well m, and ρ is the correlation coefficient used to introduce some dependence between controls of individual wells at different control time steps. Since the AR(1) model is stationary, then $\rho \in (-1, 1)$. This formulation (in addition to using the symmetric property of covariance matrix) gives a block diagonal matrix, $\mathbf{C}_\mathbf{u}^1$ of the form

$$\mathbf{C}_\mathbf{u}^1 = \begin{pmatrix} \mathbf{C}_{\mathbf{u}^1}^1 & 0 & 0 & \dots & 0 \\ 0 & \mathbf{C}_{\mathbf{u}^2}^1 & 0 & \dots & 0 \\ \cdot & & & & \\ \cdot & & & & \\ \cdot & & & & \\ 0 & 0 & 0 & \dots & \mathbf{C}_{\mathbf{u}^{N_{\text{well}}}}^1 \end{pmatrix}. \tag{25}$$

In Eq. (25), $\mathbf{C}_{\mathbf{u}^m}^1$ is the user-defined covariance matrix (obtained by using Eq. (24)) to ensure some degree of correlation and smoothness on the control vector, $\mathbf{u}^m$ for the well $m = 1, 2, \dots, N_{\text{well}}$ at iteration $l = 1$; $\mathbf{u}^m = [u_1^m, u_2^m, \dots, u_{N_t}^m]$ is the vector of control variables at well m for all the N_t control time steps. For example, u_i^m denotes the control variable for well m at the ith control time step. In general, for this problem, the complete optimization unknowns (control vector) can be written as;

$$\begin{aligned} \mathbf{u} &= [\mathbf{u}^1, \mathbf{u}^2, \dots, \mathbf{u}^{N_{\text{well}}}]^\top = [\{u_n^m\}_{n=1}^{N_t} : m = 1, 2, \dots, N_{\text{well}}]^\top \\ &= [u_1, u_2, \dots, u_{N_u}]^\top \end{aligned} \tag{26}$$

where $N_u = N_{\text{well}} \times N_t$ is the total number of control variables.

At subsequent iterations, $l \neq 1$, the covariance matrices in (23) and (25) are updated using the statistical approach presented in Stordal et al. (2016) to get an improved covariance matrix, $\mathbf{C}_\mathbf{u}^{l+1}$. In the EnOpt community, this process is called the Covariance Matrix Adaptation (CMA)-EnOpt method (Fonseca et al., 2014) (we shall refer to this as simply the "standard EnOpt method"). Also, in Eq. (22), pre-multiplying $\mathbf{G}_l^\top$ by $\mathbf{C}_\mathbf{u}^l$ has shown to produce a better performance, see e.g. Amari (1998). Indeed, the product $\mathbf{C}_\mathbf{u}^l \mathbf{G}_l^T$ is the natural gradient for this problem. It is independent of the problem parameterization and accounts for gradient uncertainty.

The preconditioned approximate gradient, $\mathbf{C}_\mathbf{u}^l \mathbf{G}_l^\top$ is computed as follows; At the lth iteration, we sample N control vectors, $\mathbf{u}_{l,j}$, $j =$

$1, 2, \ldots, N$ from a multivariate normal distribution with mean equal to the lth control vector, $\mathbf{u}_l$, and covariance matrix $\mathbf{C}_{\mathbf{u}}^l$, i.e., $\mathbf{u}_{l,j} \sim \mathcal{N}(\mathbf{u}_l, \mathbf{C}_{\mathbf{u}}^l)$, $j = 1, 2, \ldots, N$, where N is the number of perturbations. Here, the subscript j is used to identify the perturbation vector, $\mathbf{u}_{l,j}$ and hence separate it from the one obtained by optimization iteration (see Eq. (22)). Each perturbation vector, $\mathbf{u}_{l,j}, j = 1, 2, \ldots, N$ is then coupled with the penalty parameter r_k to compute the penalty function values, $P_k(\mathbf{u}_{l,j}, r_k), j = 1, 2, \ldots, N$ (see Eq. (15)). Next, we utilize the perturbations to compute the approximate sample cross-covariance of the control vector $\mathbf{u}_l$ and the objective function $P_k(u_l, r_k)$ as follows (Fonseca et al., 2017):

$$\mathbf{C}^l_{\mathbf{u},P_k(\mathbf{u},r_k)} \approx \frac{1}{N-1}\sum_{j=1}^{N}(\mathbf{u}_{l,j} - \mathbf{u}_l)\Big(P_k(\mathbf{u}_{l,j}, r_k) - P_k(\mathbf{u}_l, r_k)\Big). \tag{27}$$

Note that, in this case, we have used the fact that the mean of $\{\mathbf{u}_{l,j}\}_{j=1}^N$ can be approximated by $\mathbf{u}_l$, since

$$\mathbf{u}_{l,j} \sim \mathcal{N}(\mathbf{u}_l, \mathbf{C}^l_{\mathbf{u}}),\ j = 1, 2, \ldots, N.$$

By first order Taylor series expansion of $P_k(\mathbf{u}, r_k)$ about $\mathbf{u}_l$, one can easily show that Eq. (27) is an approximation of $\mathbf{C}^l_{\mathbf{u}}\mathbf{G}_l^{\mathsf{T}}$. Since r_k is fixed, then it is not hard to see (by Taylor expansion about $\mathbf{u}_l$) that,

$$\begin{aligned} P_k(\mathbf{u}, r_k) &= P_k(\mathbf{u}_l, r_k) + \left[\frac{\partial P_k(\mathbf{u}_l, r_k)}{\partial \mathbf{u}}\right]^{\mathsf{T}}(\mathbf{u} - \mathbf{u}_l) + O(\|(\mathbf{u} - \mathbf{u}_l)\|^2) \\ \implies P_k(\mathbf{u}, r_k) - P_k(\mathbf{u}_l, r_k) &= \left[\frac{\partial P_k(\mathbf{u}_l, r_k)}{\partial \mathbf{u}}\right]^{\mathsf{T}}(\mathbf{u} - \mathbf{u}_l) + O(\|(\mathbf{u} - \mathbf{u}_l)\|^2). \end{aligned} \tag{28}$$

Pre-multiply both sides of (28) by $(\mathbf{u} - \mathbf{u}_l)$ and set $\mathbf{u} = \mathbf{u}_{l,j}$, we get

$$\begin{aligned} &(\mathbf{u}_{l,j} - \mathbf{u}_l)(P_k(\mathbf{u}_{l,j}, r_k) - P_k(\mathbf{u}_l, r_k)) \\ &\quad = (\mathbf{u}_{l,j} - \mathbf{u}_l)\mathbf{G}_l^{\mathsf{T}}(\mathbf{u}_{l,j} - \mathbf{u}_l) + O(\|(\mathbf{u}_{l,j} - \mathbf{u}_l)\|^3), \quad \forall j = 1, 2, \ldots, N, \end{aligned} \tag{29}$$

where, $\mathbf{G}_l^{\mathsf{T}} = \frac{\partial P_k(\mathbf{u}_l, r_k)}{\partial \mathbf{u}}$ is the value of the approximate gradient of P_k at $(\mathbf{u}_l, r_k)$ and $O(\|(\mathbf{u}_{l,j} - \mathbf{u}_l)\|^3)$ is the remaining terms containing higher order (≥ 3) of $(\mathbf{u}_{l,j} - \mathbf{u}_l)$. Assuming that the magnitude of the difference, $(\mathbf{u}_{l,j} - \mathbf{u}_l)$ is very small, then with first order Taylor expansion (by neglecting, $O(\|(\mathbf{u}_{l,j} - \mathbf{u}_l)\|^3)$), we obtain the following from (29).

$$\begin{aligned} &\frac{1}{N-1}\sum_{j=1}^{N}(\mathbf{u}_{l,j} - \mathbf{u}_l)(P_k(\mathbf{u}_{l,j}, r_k) - P_k(\mathbf{u}_l, r_k)) \\ &\qquad \approx \Big(\frac{1}{N-1}\sum_{j=1}^{N}(\mathbf{u}_{l,j} - \mathbf{u}_l)(\mathbf{u}_{l,j} - \mathbf{u}_l)\Big)G_l^{\mathsf{T}} \\ \implies &\mathbf{C}^l_{\mathbf{u},P_k(\mathbf{u},r_k)} \approx \mathbf{C}^l_{\mathbf{u}}\mathbf{G}_l^{\mathsf{T}}. \end{aligned} \tag{30}$$

The iterative scheme of the EnOpt (see Eq. (22)) is repeated until a specified stopping (or convergence) criteria is satisfied. In this study, we used the following criteria

$$\frac{|P_k(\mathbf{u}_{l+1}, r_k) - P_k(\mathbf{u}_l, r_k)|}{|P_k(\mathbf{u}_l, r_k)|} < \epsilon_3, \tag{31}$$

where ϵ_3 is a specified tolerance.

3.1.1. Backtracking line search method

The backtracking method (similar to the one in Nocedal and Wright (2006)) considered in this study is demonstrated in Algorithm 1 (the Armijo condition for sufficient decrease).

Algorithm 1: Procedure for step size selection

Step 1. Fix parameters $\alpha_1 \in (0, 1)$ and $\alpha_2 \in (0, 1)$.
Step 2. Start iteration with step size $\lambda := \frac{1}{\beta_1} > 0$.
while $P(\mathbf{u}_{l+1}, r_k) \geq P(\mathbf{u}_l, r_k) - \alpha_2\lambda\nabla_{\mathbf{u}}^{\mathsf{T}}P(\mathbf{u}_l, r_k)\mathbf{g}_l$ **do**
  $\lambda = \alpha_1\lambda$
end while

In Algorithm 1, $\mathbf{g}_l$ is the search direction at the lth iteration evaluated using,

$$\mathbf{g}_l = \frac{\nabla_{\mathbf{u}}^{\mathsf{T}}P(\mathbf{u}_l, r_k)}{\|\nabla_{\mathbf{u}}^{\mathsf{T}}P(\mathbf{u}_l, r_k)\|_2},$$

$\nabla_{\mathbf{u}}^{\mathsf{T}}P(\mathbf{u}_l, r_k)$ is the regularized approximate gradient of $P(\mathbf{u}_l, r_k)$ computed using Eq. (27), α_1 is the backstepping or step size contraction parameter, and α_2 is a given constant. From vector dot product, it is clear that,

$$\begin{aligned} \nabla_{\mathbf{u}}^{\mathsf{T}}P(\mathbf{u}_l, r_k)\mathbf{g}_l &= \|\nabla_{\mathbf{u}}^{\mathsf{T}}P(\mathbf{u}_l, r_k)\|_2\|\mathbf{g}_l\|_2\cos\theta \\ &= \|\nabla_{\mathbf{u}}^{\mathsf{T}}P(\mathbf{u}_l, r_k)\|_2\left\|\frac{\nabla_{\mathbf{u}}^{\mathsf{T}}P(\mathbf{u}_l, r_k)}{\nabla_{\mathbf{u}}^{\mathsf{T}}P(\mathbf{u}_l, r_k)}\right\|_2\cos\theta \\ \implies \nabla_{\mathbf{u}}^{\mathsf{T}}P(\mathbf{u}_l, r_k)\mathbf{g}_l &= \|\nabla_{\mathbf{u}}^{\mathsf{T}}P(\mathbf{u}_l, r_k)\|_2, \quad (\text{since } \theta = 0) \end{aligned} \tag{32}$$

where θ is the angle between the vectors $\nabla_{\mathbf{u}}^{\mathsf{T}}P(\mathbf{u}_l, r_k)$ and $\mathbf{g}_l$. Therefore, for convenience, we utilize Eq. (32) in Algorithm 1.

4. EPF-EnOpt method

The combined strategies of the Exterior PF method with the EnOpt method give rise to a more accurate and robust optimal solution method, the EPF-EnOpt method, for constrained optimization problems. More concisely, we present the workflow of the EPF-EnOpt procedures in Algorithm 2.

Algorithm 2: Procedures for solving constrained optimization problems

Step 1. Given tolerances $\epsilon_1 > 0$ and $\epsilon_2 > 0$, a suitable initial penalty parameter $r_1 > 0$, and a growth constant $c \geq 1$, initial starting point (feasible or infeasible) $\mathbf{u}_1 := \mathbf{u}(r_1) \in \mathbb{R}^{N_u}$. Set $k = 1$.
Step 2. Formulate the term, P_k of the sequence $\{P_k\}_{k=1}^{\infty}$, using Eq. (15).
Step 3. Find a solution $\mathbf{u}_k^* := \mathbf{u}^*(r_k)$ of the unconstrained minimization problem stated in Eq. (21) using the EnOpt procedures (in sub-section 3.1).
Step 4. Check the stopping criteria:
if $|P_k(\mathbf{u}^*(r_k)) - P_k(\mathbf{u}(r_k))| < \epsilon_1$ **then**
  if $|Q(\mathbf{u}^*(r_k))| \leq \epsilon_2$ **then**
    set, $\mathbf{u}^* = \mathbf{u}_k^*$ ($\mathbf{u}^*$ is the solution of the original problem (5)–(7)) and terminate;
  else
    go to Step 5
  end if
else
  go to Step 5
end if
Step 5. Select $r_{k+1} = cr_k, \mathbf{u}_{k+1} = \mathbf{u}_k^*$. Set $k = k + 1$, and turn to Step 2.

4.1. Convergence of the EPF method

In this section, we consider the problem (5)–(7) where f, $g_i, \forall i \in \mathrm{I}$, and $h_j, \forall j \in \mathrm{E}$ are continuous functions defined on $\mathbb{R}^{N_u}$ and a sequence of penalty parameters, $\{r_k\}_{k=1}^{\infty}$ that satisfies the condition of Eq. (16). Assume that for each $k = 1, 2, \ldots$, $\mathbf{u}_k^* := \mathbf{u}^*(r_k)$ is the optimal solution (or the desired minimizer) of the unconstrained optimization problem (21). Also, we assume that the desired optimal solution, $\mathbf{u}^*$ of the original constrained optimization problem (5)–(7) exist and is unique. We establish in Lemma 4.1, the basic properties of the exterior PF formulation, and the proof of convergence of the EPF procedures is thereafter presented.

Lemma 4.1. *Suppose that $\{r_k\}_{k=1}^{\infty}$ is a strictly increasing sequence, i.e. $0 < r_k < r_{k+1}, \forall k = 1, 2, \ldots$, then*

1. $P_k(\mathbf{u}_k^*) \le P_{k+1}(\mathbf{u}_{k+1}^*)$,
2. $f(\mathbf{u}_k^*) \le f(\mathbf{u}_{k+1}^*)$,
3. $Q(\mathbf{u}_k^*) \ge Q(\mathbf{u}_{k+1}^*)$.

Proof.

1. Using the definition of $P_k, k = 1, 2, \ldots$, in Eq. (15) and since $\mathbf{u}_k^*$ and $\mathbf{u}_{k+1}^*$ are the minimizers of P_k and P_{k+1} respectively, we have

$$P_k(\mathbf{u}_k^*) \le P_k(\mathbf{u}_{k+1}^*), \tag{33}$$

and

$$P_{k+1}(\mathbf{u}_{k+1}^*) \le P_{k+1}(\mathbf{u}_k^*). \tag{34}$$

Because, $r_k, k = 1, 2, \ldots$, is an increasing sequence, then

$$P_k(\mathbf{u}_{k+1}^*) \le P_{k+1}(\mathbf{u}_{k+1}^*). \tag{35}$$

It follows from inequalities (33) and (35) that

$$P_k(\mathbf{u}_k^*) \le P_{k+1}(\mathbf{u}_{k+1}^*), \quad \forall k = 1, 2, \ldots, \tag{36}$$

Hence, the proof of Statement 1.

2. Divide both sides of inequalities (33) and (34) by r_k and r_{k+1}, respectively to obtain,

$$\begin{aligned}
&\frac{1}{r_k} P_k(\mathbf{u}_k^*) \le \frac{1}{r_k} P_k(\mathbf{u}_{k+1}^*) \\
&\implies \frac{1}{r_k}\left(f(\mathbf{u}_k^*) + r_k Q(\mathbf{u}_k^*)\right) \le \frac{1}{r_k}\left(f(\mathbf{u}_{k+1}^*) + r_k Q(\mathbf{u}_{k+1}^*)\right) \\
&\quad \text{(using the definition of } P_k) \\
&\implies \frac{1}{r_k} f(\mathbf{u}_k^*) + Q(\mathbf{u}_k^*) \le \frac{1}{r_k} f(\mathbf{u}_{k+1}^*) + Q(\mathbf{u}_{k+1}^*)
\end{aligned} \tag{37}$$

and

$$\begin{aligned}
&\frac{1}{r_{k+1}} P_{k+1}(\mathbf{u}_{k+1}^*) \le \frac{1}{r_{k+1}} P_{k+1}(\mathbf{u}_k^*) \\
&\implies \frac{1}{r_{k+1}}\left(f(\mathbf{u}_{k+1}^*) + r_{k+1} Q(\mathbf{u}_{k+1}^*)\right) \le \frac{1}{r_{k+1}}\left(f(\mathbf{u}_k^*) + r_{k+1} Q(\mathbf{u}_k^*)\right) \\
&\implies \frac{1}{r_{k+1}} f(\mathbf{u}_{k+1}^*) + Q(\mathbf{u}_{k+1}^*) \le \frac{1}{r_{k+1}} f(\mathbf{u}_k^*) + Q(\mathbf{u}_k^*).
\end{aligned} \tag{38}$$

Adding inequalities (37) and (38) and rearranging the result, we get

$$\left(\frac{1}{r_k} - \frac{1}{r_{k+1}}\right) f(\mathbf{u}_k^*) \le \left(\frac{1}{r_k} - \frac{1}{r_{k+1}}\right) f(\mathbf{u}_{k+1}^*). \tag{39}$$

Recall from the definition of r_k that for each $k = 1, 2, \ldots$,

$$r_k < r_{k+1} \implies \frac{1}{r_k} > \frac{1}{r_{k+1}} \implies \frac{1}{r_k} - \frac{1}{r_{k+1}} > 0. \tag{40}$$

Using (40), we can easily divide both sides of the inequality (39) by $(\frac{1}{r_k} - \frac{1}{r_{k+1}})$ to obtain

$$f(\mathbf{u}_k^*) \le f(\mathbf{u}_{k+1}^*). \tag{41}$$

Thus the statement 2. holds for any $k = 1, 2, \ldots,$.

3. Adding inequalities (33) and (34) gives

$$\begin{aligned}
&P_k(\mathbf{u}_k^*) + P_{k+1}(\mathbf{u}_{k+1}^*) \le P_k(\mathbf{u}_{k+1}^*) + P_{k+1}(\mathbf{u}_k^*) \\
&\implies P_k(\mathbf{u}_k^*) - P_{k+1}(\mathbf{u}_k^*) - \left(P_k(\mathbf{u}_{k+1}^*) - P_{k+1}(\mathbf{u}_{k+1}^*)\right) \le 0 \\
&\implies r_k Q(\mathbf{u}_k^*) - r_{k+1} Q(\mathbf{u}_k^*) - \left(r_k Q(\mathbf{u}_{k+1}^*) - r_{k+1} Q(\mathbf{u}_{k+1}^*)\right) \le 0 \\
&\implies (r_k - r_{k+1}) Q(\mathbf{u}_{k+1}^*) \ge (r_k - r_{k+1}) Q(\mathbf{u}_k^*).
\end{aligned} \tag{42}$$

Since, $r_k < r_{k+1} \implies r_k - r_{k+1} < 0$, then dividing both sides of the inequality (42) by $(r_k - r_{k+1})$, a negative value, reverses the inequality sign and hence leads to

$$Q(\mathbf{u}_k^*) \ge Q(\mathbf{u}_{k+1}^*), \tag{43}$$

This completes the proof of Statement 3. Also, this confirms the fact that for any initial infeasible solution $\mathbf{u}_k^*$, the next approximate solution $\mathbf{u}_{k+1}^*$ obtain by the Algorithm 2 is indeed an improved solution (less infeasible), and would eventually lead to feasible solution as $r_k \to +\infty$ as shown in the next theorem. □

Theorem 4.2 (*Convergence Theorem*). *Let D be the set of feasible solutions to the given constrained optimization problem (5)–(7). Suppose that the penalty function $P_k(\mathbf{u}, r_k)$ is sequentially minimized for a strictly increasing sequence of penalty parameters $r_k, k = 1, 2, \ldots$, i.e., for any fixed k, the optimal solution, $\mathbf{u}_k^*$ of the subproblem (21) becomes the initial starting point for the subproblem at $k = k + 1$, with $r_{k+1} > r_k$. If the sequence of the unconstrained minima, $\{\mathbf{u}_k^*\}_{k=1}^{\infty}$ converges, then its limit is the desired optimum, $\mathbf{u}^* \in D$ of the original constrained problem (5)–(7) and $Q(\mathbf{u}_k^*) \to 0$ as $k \to +\infty$ respectively.*

Proof. Assume that $\{\mathbf{u}_k^*\}_{k=1}^{\infty}$ has a convergent subsequence whose limit is $\bar{\mathbf{u}}^*$ in $\mathbb{R}^{N_u}$. Hence,

$$\lim_{k \to +\infty} \mathbf{u}_k^* = \bar{\mathbf{u}}^*. \tag{44}$$

We need to show that $\bar{\mathbf{u}}^*$ is feasible to the original constrained optimization problem (5)–(7) and that $\mathbf{u}^* = \bar{\mathbf{u}}^*$. Since for each $k = 1, 2, \ldots$, $\mathbf{u}_k^*$ is the optimal solution of $P_k(u, r_k)$, then the following holds:

$$\begin{aligned}
&f(\mathbf{u}_k^*) \le f(\mathbf{u}_k^*) + r_k Q(\mathbf{u}_k^*) = P_k(\mathbf{u}_k^*, r_k) \le P_k(\mathbf{u}^*, r_k) = f(\mathbf{u}^*) \\
&\qquad (\text{since}, \quad Q(\mathbf{u}^*) = 0)
\end{aligned} \tag{45}$$

$$\implies f(\mathbf{u}_k^*) \le f(\mathbf{u}^*). \tag{46}$$

Also from the inequality (45), we have

$$r_k Q(\mathbf{u}_k^*) \le f(\mathbf{u}^*) - f(\mathbf{u}_k^*) \implies Q(\mathbf{u}_k^*) \le \frac{1}{r_k}\left(f(\mathbf{u}^*) - f(\mathbf{u}_k^*)\right) \tag{47}$$

Taking the limit as $k \to +\infty$ on both sides of the inequality (47), we get

$$\begin{aligned}
&\lim_{k \to +\infty} Q(\mathbf{u}_k^*) \le \lim_{k \to +\infty} \frac{1}{r_k}\left(f(\mathbf{u}^*) - f(\mathbf{u}_k^*)\right) = 0 \qquad \left(\text{since}, \quad \lim_{k \to +\infty} \frac{1}{r_k} = 0\right) \\
&\implies \lim_{k \to +\infty} Q(\mathbf{u}_k^*) \le 0 \implies Q(\lim_{k \to +\infty} \mathbf{u}_k^*) \le 0 \\
&\implies Q(\bar{\mathbf{u}}^*) \le 0 \quad (\text{using Eq. (44)}).
\end{aligned} \tag{48}$$

It follows from (20) and (48) that

$$Q(\bar{\mathbf{u}}^*) = 0. \tag{49}$$

Hence, $\bar{\mathbf{u}}^*$ is feasible (i.e., $\bar{\mathbf{u}}^* \in D$) to the original problem (5)–(7). By the definition of $\mathbf{u}^*$, then,

$$f(\mathbf{u}^*) \le f(\bar{\mathbf{u}}^*) \tag{50}$$

Since f is continuous and monotone increasing with respect to $\mathbf{u}^*(r_k)$ (according to Statement 3 of Lemma 4.1), taking the limit as $k \to +\infty$ on both sides of (46) gives

$$\lim_{k \to +\infty} f(\mathbf{u}_k^*) = f(\bar{\mathbf{u}}^*) \le f(\mathbf{u}^*) \tag{51}$$

Using inequalities (50) and (51) lead to

$$f(\mathbf{u}^*) = f(\bar{\mathbf{u}}^*). \tag{52}$$

Thus, $\bar{\mathbf{u}}^*$ is the desired optimal solution of the original problem (5)–(7). This concludes the proof of the fact that the sequence $\{\mathbf{u}_k^*\}_{k=1}^{\infty}$ converges to the optimal solution $\mathbf{u}^*$ as $k \to +\infty$. □

5. Applications

In this section, we utilize numerical results to compare the convergence rate and accuracy of the standard EnOpt method with our proposed EPF-EnOpt method. We examine the two optimal solution methods by solving one analytical problem, and one simple water flooding constrained optimization problem.

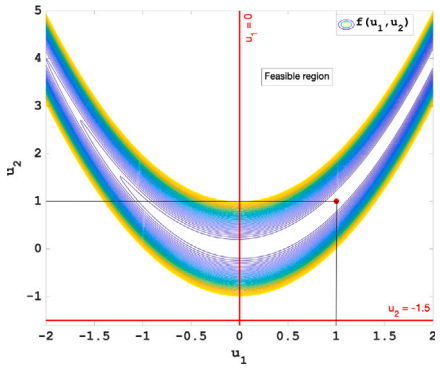

Fig. 1. The contour plot of the objective function in Eq. (53) and its global minimum point in the feasible region.

Example 1

Here, we consider a classical constrained 2D Rosenbrock's optimization problem (also called the Hock & Schittkowski problem 1 (Hock and Schittkowski, 1981; Snyman and Wilke, 2018)) with an additional constraint on the variable u_1. The problem is given as follows.

$$\min_{\mathbf{u}\in\mathbb{R}^2} \; f(\mathbf{u}) = 100(u_2 - u_1^2)^2 + (1-u_1)^2 \tag{53}$$

subject to: $u_1 \geq 0.$ (54)

$$u_2 + 1.5 \geq 0, \tag{55}$$

where $\mathbf{u} = [u_1, u_2]^\mathsf{T}$. By considering a point $\mathbf{u} = [0,1]^\mathsf{T}$ in the feasible region, we see that the Hessian of the objective function $f(\mathbf{u})$ given by

$$\nabla^2 f(\mathbf{u}) = \begin{bmatrix} 1200u_1^2 - 400u_2 + 2 & -400u_1 \\ -400u_1 & 200 \end{bmatrix} \tag{56}$$

has a negative eigenvalue (and thus, the Hessian of f is not positive definite). This shows that the function is non-convex in the feasible region, and hence in the entire $\mathbb{R}^2$. Because of this, convergence to the global minimizer of the problem (53)–(55) using a numerical minimization procedure can be difficult to achieve. However, an approximation can be found. In theory, the global minimum value of the problem (53)–(55) is at the point $u_1 = 1$ and $u_2 = 1$ as shown in Fig. 1.

First, we apply the standard adaptive EnOpt method of Section 3.1 and the linear transformation of subsection 2.1 to find the solution of problem (53)–(55). In this case, we choose an initial guess $\mathbf{u}_1 = [-2, 0.5]^\mathsf{T}$ (see Fig. 2(b)), the initial step size, β_1^{-1} is set to 0.5. The initial perturbation size for each variable is taken as 0.05 (in other to compute the initial covariance matrix (23)), and the initial step size for covariance adaptation is set to 0.1. Here, we used $N = 100$ perturbation control vectors at each iteration and set $\epsilon_3 = 1.0\times10^{-6}$ as the tolerance for convergence. The backtracking parameters, α_1 & α_2 are chosen as 0.5 and 0.001 respectively. The maximum number of trials for the process of backtracking (see Algorithm 1) is set to 20. To use the linear transformation, we set the upper limit, $u_i^{\text{upp}} = 5$ for each variable $u_i, i = 1, 2$. After 600 iterations, the standard EnOpt procedure converges (for which $|f(\mathbf{u}_{l+1}) - f(\mathbf{u}_l)| \leq \epsilon_3 |f(\mathbf{u}_l)|$ is sufficiently satisfied) to the minimum point as shown in Fig. 2(a). Fig. 2(b) further illustrates, on a contour plot, the convergence of the corresponding objective function values (in blue dots) at optimization iterations to its minimum (in red dot) in the feasible region.

However, the large iterations required before convergence to the solution of problem (53)–(55) by using the standard EnOpt method can be significantly reduced by using the proposed EPF-EnOpt method presented in Algorithm 2. To utilize the EPF-EnOpt Algorithm 2 for this example, first, we construct the general term of the penalty function sequence in (15) as follows:

$$\begin{aligned} P_k(\mathbf{u}(r_k)) &= f(\mathbf{u}(r_k)) + r_k Q(\mathbf{u}(r_k)), \qquad k = 1, 2, \ldots, \\ &= 100(u_2(r_k) - u_1(r_k)^2)^2 + (1 - u_1(r_k))^2 \\ &\quad + r_k\big((\min\{u_1(r_k), 0\})^2 + (\min\{(u_2(r_k) + 1.5), 0\})^2\big), \end{aligned} \tag{57}$$

where $\mathbf{u}(r_k) = [u_1(r_k), u_2(r_k)]^\mathsf{T}$ denotes a value of $\mathbf{u}$ at a given penalty parameter r_k (Note that, the subproblem associated with (57) according to Eq. (21) shall simply be called the "subproblem P_k"). We set the initial penalty parameter, r_1 and the growth constant, c to 1.5 respectively and choose $\epsilon_1 = 1.0 \times 10^{-6}$ and $\epsilon_2 = 1.0 \times 10^{-6}$. Similarly, we utilize an infeasible initial guess $\mathbf{u}(r_1) = [-2, 0.5]^\mathsf{T}$ (see Fig. 3(b)). For the purpose of results comparison, same initialization (as before) of parameters in the EnOpt procedures are used (in Step 3 of Algorithm 2). In addition, we normalize each variable $u_i(r_k), i = 1, 2$ using the same linear transformation of subsection 2.1 (without truncation) with $u_i^{\text{upp}} = 5, \forall i = 1, 2$. However, we note that normalizing the variables this way is not compulsory as one could use a fixed constant or the maximum of the variables. On the application of Algorithm 2, the resulting successive minimum points (including the initial starting point) of the penalty function terms (or subproblems) in the sequence P_k, $k = 1, 2, 3, \ldots, 24$ are presented in Fig. 3(a). Here, we found that, the Algorithm 2 converges to the minimum of problem (53)–(55) after the solution of the subproblem P_{24}. The total number of unconstrained minimization iterations (from the starting point) before convergence is 52 as shown in Fig. 4. Fig. 3(b) depicts the corresponding values (in blue dots) of the objective function (53) at the initial guess and the obtained minimum points of subproblems $\{P_k\}_{k=1}^{24}$ respectively. From the numerical optimization results of this example, we see that the EPF-EnOpt method gives a faster convergence rate and also more accurate results than the standard EnOpt method.

For this example, the large number of iterations required by standard EnOpt method is seen as the effect of the truncation (see Eq. (9)) that often occurs with the perturbed vectors (sampled from a Gaussian distribution with adapted covariance matrix and the approximate solution (at each iteration) as the mean) and the approximate solution respectively. As pointed out in Section 2.1, the truncation affects the quality of the approximate gradient and hence a small step size is required for a decrease of the objective function. This continues at each iteration until convergence and hence the reason for a large number of iterations. Also, with different perturbation size (ranging from 0.0001 to 0.5) for each unknown variable and different updating step sizes for the covariance matrix (ranging from 0.001 to 0.1) we found no improvement in the number of iterations required for the standard EnOpt convergence.

However, in EPF-EnOpt method, infeasible perturbed vectors and iterates are kept. Instead of truncation due to infeasibility (as it is done in the standard EnOpt), the violations of the constraints are handled by the penalty term. By doing this resolves the large number of iterations required by the standard EnOpt to 52.

Example 2

In this case, we consider a practical N_u−dimensional constrained optimization problem of water flooding for a single (i.e we assume no geological uncertainty) 5-Spot oil reservoir (see Fig. 5). This is a synthetic 2D reservoir model with three-phase flow (including oil, water and gas) solved using the OPM-Flow simulator (opm-project.org). The model has a central injection and four production wells spatially distributed in a five-spot pattern as shown in Fig. 5. The reservoir model is uniformly discretized into 50 × 50 grid cells, with $\Delta x = \Delta y = 100$ m. On average, it has approximately 30% porosity with heterogeneous permeability map. The initial reservoir pressure is 200 bar. The initial average oil and water saturations are 0.6546 and 0.3454 respectively (i.e, no free gas). The original oil in place (OOIP) is 4.983×10^6 sm^3.

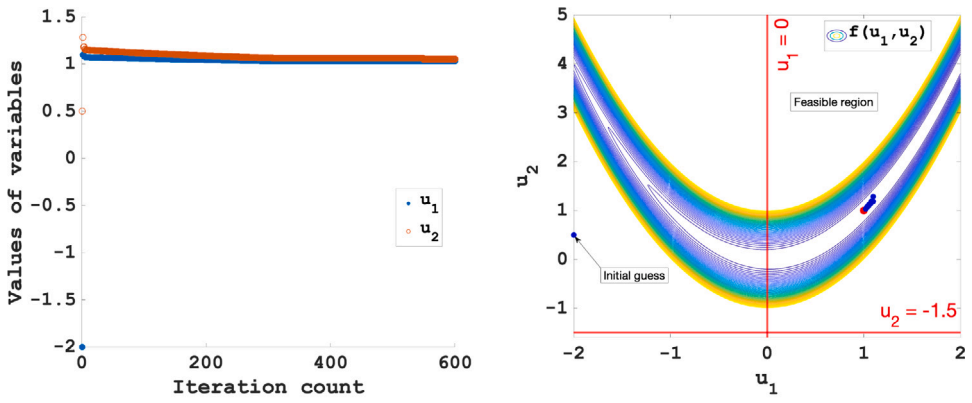

Fig. 2. Minimization of the constrained 2D Rosenbrock problem (53)–(55) using the Standard EnOpt method. (a) Plot of values of control variables versus iteration count. (b) The contour plot of the objective function (53) and its values (in blue dots) at different estimates of the control variables from optimization iterations.

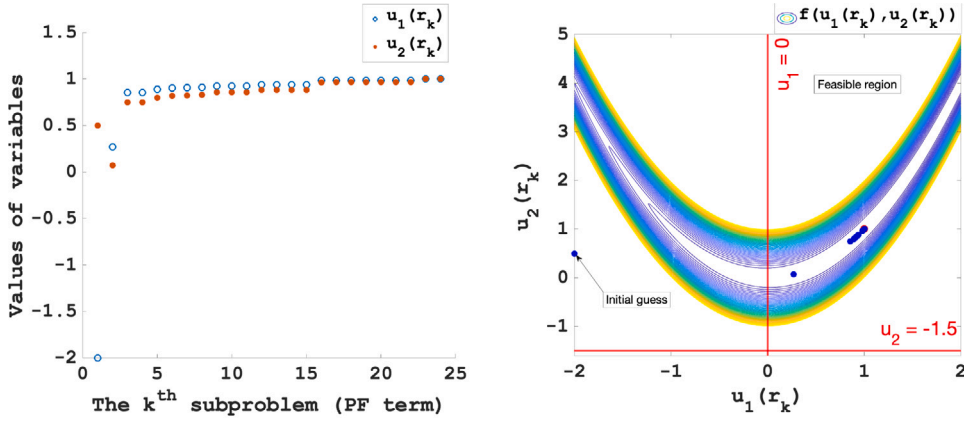

Fig. 3. Minimization of the constrained 2D Rosenbrock problem (53)–(55) using the EPF-EnOpt Algorithm. (a) Plot of the unconstrained minimum points of subproblems in the penalty function sequence. (b) The contour plot of the objective function (53) and its values (in blue dots) at the initial guess and minimum points of subproblems.

Fluid properties is close to that of a light oil reservoir. The viscosity (in cP) for saturated oil at varying bubble point pressure is in the interval $[0.1, 0.56]$ and viscosity of water is 0.01 cP. The densities of oil and water are respectively 732 kg/m^3 and 1000 kg/m^3. The optimization problem is to find the best/ optimum $\mathbf{u} \in \mathbb{R}^{N_u}$ that maximizes the net present value (NPV) defined by the objective function:

$$J(\mathbf{u}) = \sum_{i=1}^{N_t} \frac{r_o Q_{o,i}(\mathbf{u}) + r_g Q_{g,i}(\mathbf{u}) - \left(r_{wi} Q_{w,i}(\mathbf{u}) + r_{wp} Q_{wp,i}(\mathbf{u})\right)}{(1+d_\tau)^{\frac{t_i}{\tau}}}, \tag{58}$$

subject to

$$u_i^{\text{low}} \le u_i \le u_i^{\text{upp}}, \quad \forall i = 1, 2, \ldots, N_u, \tag{59}$$

where N_t is the total control time steps; i is the index for time step; d_τ is the discount rate (decimal %) for a given period of time τ (days), and t_i is the cumulative time (days) starting from the beginning of production up to the ith time step; the scalars r_o, r_{wi}, r_{wp}, and r_g denote the price of oil, the cost of handling water injection and production, and the price of gas production (in USD/sm^3) respectively. Let Δt_i be the length of time (days) between t_i and the t_{i-1} time steps. In Eq. (58), $Q_{w,i}$ is the total water injection (sm^3) over the time interval Δt_i; $Q_{o,i}, Q_{wp,i}$, and $Q_{g,i}$ denote the total oil, water, and gas productions (sm^3) over the time interval Δt_i. Also, the quantities $Q_{o,i}, Q_{w,i}, Q_{wp,i}$, and $Q_{g,i}$ are primary variables which depend on the control vector $\mathbf{u}$ at each control time step and their respective numerical values are the results of water flooding reservoir simulation based on a given well configuration data provided by some optimization procedures. We simulated water flooding on the 5-Spot field using the OPM-Flow simulator. In Eq. (59), u_i^{low} and u_i^{upp} are the imposed lower and upper bounds on the control variable u_i, $\forall i = 1, 2, \ldots, N_u$.

In this example, the injection well is controlled by water injection rate at each control time step. The lower and upper bounds for water injection rate are set to 0 sm^3/day and 1000 sm^3/day respectively. Each production well is controlled by reservoir fluid production rate with a lower limit of 0 sm^3/day and upper limit of 250 sm^3/day. Bottom hole pressure (BHP) limits are imposed on the wells, specifically maximum 500 bar for the injector and minimum 150 bar for each producer. The simulation period for the reservoir is 1500 days and the control time step is set to 30 days. Therefore, the optimization unknown control vector $\mathbf{u}$ has a total of $(1+4) \times 50 = 250$ components (control variables). The values of economic parameters utilized for this optimization problem is given by Table 2.

The constrained water flooding optimization (maximization) problem (58)–(59) is treated as a minimization problem by using the transformation in Eq. (4). Next, we seek a solution to the transformed problem, first by using the standard EnOpt approach (see Section 3.1) coupled with the linear transformation (with truncation) of Section 2.1. Here, we select an initial feasible guess, $\mathbf{u}_1$ of control vector (denoted by the "ref control" in Fig. 6). Namely, a constant 500 sm^3/day for the water injection rate at the injection well, and 150 sm^3/day for the reservoir fluid production rate target at each production well. The values of other optimization parameters considered in the EnOpt algorithm

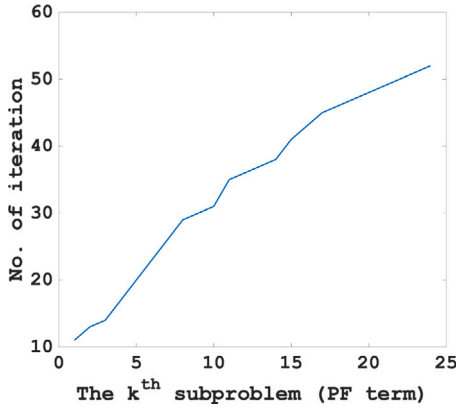

Fig. 4. Plot of cumulative number of unconstrained minimization iterations versus the kth subproblem for the 2D Rosenbrock problem.

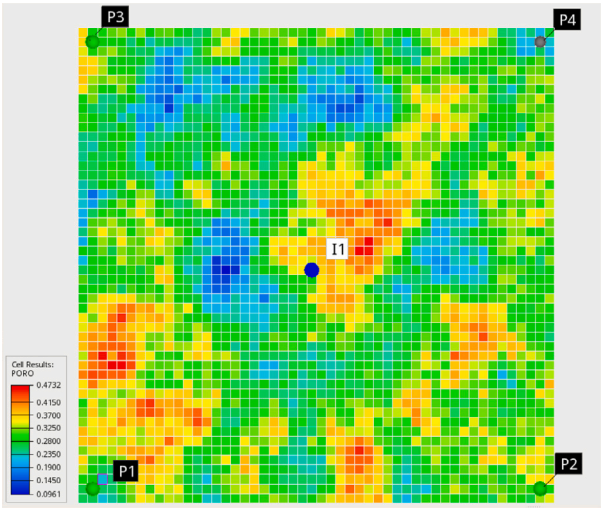

Fig. 5. Porosity distribution of the five-spot field.

are given in Table 1. After 20 iterations, the standard EnOpt algorithm converges (when $|J(\mathbf{u}_{l+1}) - J(\mathbf{u}_l)| \leq \epsilon_3 |J(\mathbf{u}_l)|$ is sufficiently satisfied) to a suboptimal solution (represented by the "standard EnOpt" in Fig. 6) of the problem (58)–(59). The maximum NPV reached is 3.855×10^8 (in USD) (see the "standard EnOpt" in Fig. 7(a)).

Furthermore, we used the proposed EPF-EnOpt method (in Algorithm 2) to solve the equivalent minimization problem associated with problem (58)–(59) in other to demonstrate its added advantage in the hydrocarbon industries. First, we rewrite the bound constraint inequalities (59) in the preferred standard form (of inequalities (6)) as follows:

$$g_1(u_i) := u_i - u_i^{low} \geq 0, \quad \text{and} \quad g_2(u_i) := u_i^{upp} - u_i \geq 0, \quad \forall i = 1, 2, \ldots, N_u. \tag{60}$$

By using Eqs. (58) and (60), the general PF term associated with problem (58)–(59) is then formulated as follows:

$$\begin{aligned} P_k(\mathbf{u}(r_k)) &= f(\mathbf{u}(r_k)) + r_k Q(\mathbf{u}(r_k)), \qquad k = 1, 2, \ldots, \\ &= f(\mathbf{u}(r_k)) \\ &\quad + r_k \Big(\sum_{i=1}^{N_u} (\min\{g_1(u_i(r_k)), 0\})^2 + \sum_{i=1}^{N_u} (\min\{g_2(u_i(r_k)), 0\})^2 \Big), \end{aligned} \tag{61}$$

where $f(\mathbf{u}(r_k)) = -J(\mathbf{u}(r_k))$. Next, we set the initial penalty parameter, r_1 and the growth constant, c to 0.1 and 10 respectively, and $\epsilon_1 = 1.0 \times 10^{-5}$ and $\epsilon_2 = 1.0 \times 10^{-6}$. The initial guess of solution is taken as $\mathbf{u}(r_1) := \mathbf{u}_1$ (see the "Ref control" in Fig. 6). We used the values of parameters in Table 1 required for the unconstrained minimization procedures. We apply the linear transformation (without truncation) of subsection 2.1 to normalize each unknown variable $u_i, i = 1, 2, \ldots, N_u$ (and hence the associated constraint function). On the application of Algorithm 2, the resulting limit of the solutions of subproblems P_k, $k = 1, 2, 3, \ldots, 26$ (equivalently the solution of problem (58)–(59)) is represented by the "EPF-EnOpt" in Fig. 6. The corresponding value of the objective function (58) at the solution of subproblem, $P_k, k = 1, 2, \ldots, 26$ is denoted by the "EPF-EnOpt" in Fig. 7(a). In this case, the Algorithm 2 is seen to converge to a better suboptimal solution of problem (53)–(55) at the 24th subproblem with a total of 51 unconstrained optimization iterations as shown in Fig. 8. The maximum NPV obtained is 4.420×10^8 (in USD). Therefore, the EPF-EnOpt method yields an increase of 14.596% in NPV over the standard

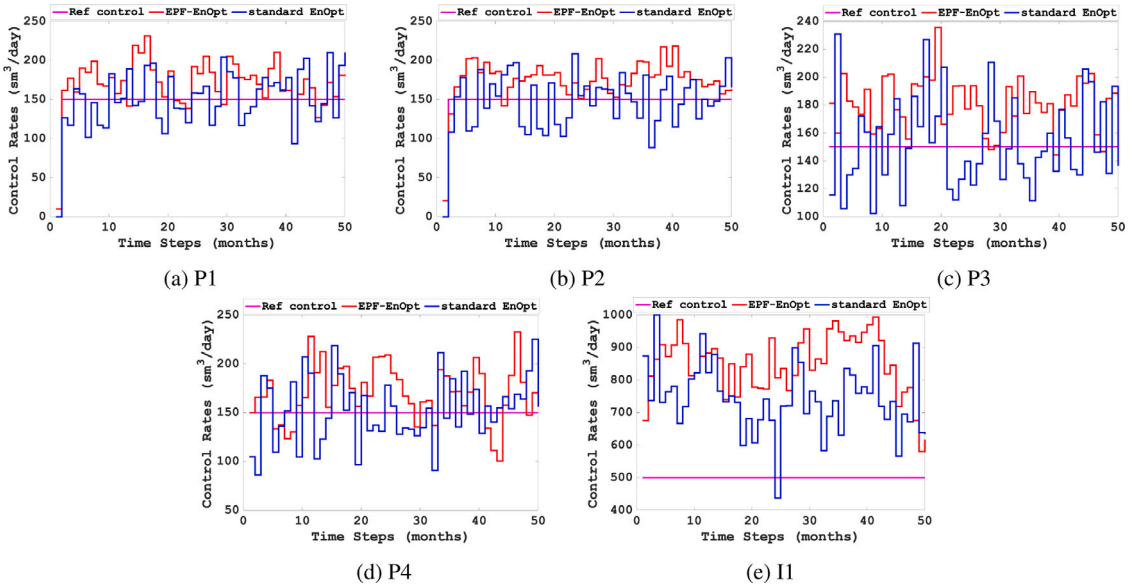

Fig. 6. Comparison of the initial (ref) and optimal solutions from standard EnOpt and EPF-EnOpt methods for the optimization problem (58)–(59). Plots (a) to (d) represent the control (production rate) variation profiles at the four producing wells and (e) denotes the control (injection rate) variation profile at the injection well I1.

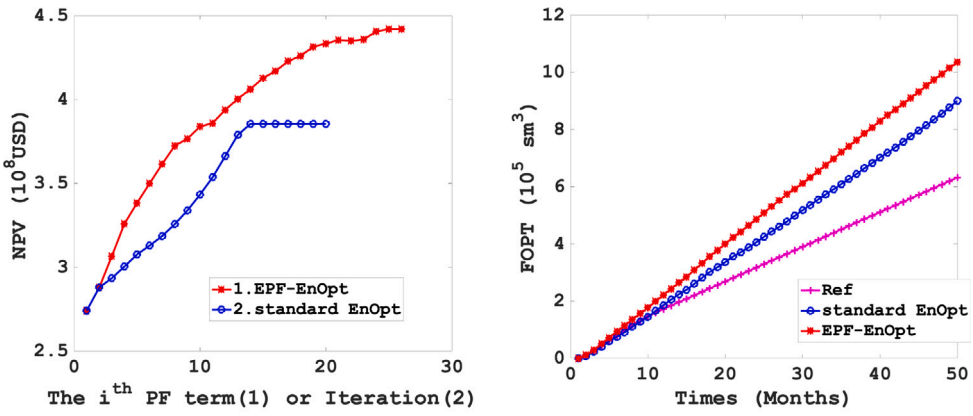

(a) NPV variation (b) Field Oil Production Total

Fig. 7. (a) Comparison of the change in NPV with iteration (for standard EnOpt) or penalty function term (or subproblem). We see that the objective function is flatting out for both methods, which indicate that the stopping criteria is sufficient for this problem. (b) Comparison of the field oil production total (FOPT) from reference (Ref), standard EnOpt, and EPF-EnOpt controls.

Table 1
Standard EnOpt parameters.

Parameter	Value
Initial step size (β_1^{-1})	0.3
Initial stepsize for covariance adaptation ($-$)	0.1
step size contraction (α_1)	0.5
Constant (α_2)	0.01
Initial control-type variance ($\sigma_m, \forall m = 1, 2, \ldots, 5$)	0.001
Number of perturbation control vector (N)	50
Constant correlation factor (ρ)	0.5
Tolerance for EnOpt convergence (ϵ_3)	10^{-6}

Table 2
Economic parameters.

Parameter	Value	Unit
Oil price (r_o)	500	USD/sm^3
Price of gas production (r_g)	0.15	USD/sm^3
Cost of water injection or production (r_{wi}, r_{wp})	30	USD/sm^3
Annual discount rate (d_r)	0.1	–

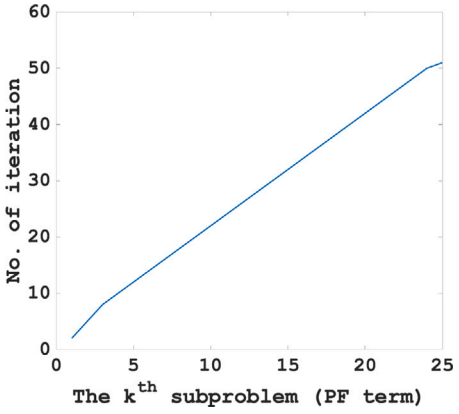

Fig. 8. Plot of cumulative number of unconstrained minimization iteration versus the kth subproblem for the 5-Spot problem.

EnOpt approach. Also, Fig. 7(b) compares the field oil production total from operating the field with the solutions (or control strategies) of the EPF-EnOpt and standard EnOpt methods respectively and the reference control. The total field oil production by the standard EnOpt and EPF-EnOpt solutions are 9.006×10^5 sm^3 and 1.036×10^6 sm^3 respectively. It is an increase of approximately 14.983% in oil production. Hence the benefit of the EPF-EnOpt method, as shown in this example is in its better and more accurate result than the traditional EnOpt scheme.

To illustrate that our proposed solution method is not significantly dependent on the state of random number generation (for objective function gradient computation), we compare its performance (in terms of change in NPV and change in cumulative unconstrained iterations) and that of standard EnOpt with different random seed numbers. Fig. 9(a) shows the changes in the maximum NPV obtained from using the EPF-EnOpt and standard EnOpt methods with different seed numbers. On average, the maximum NPV for the EPF-EnOpt and standard EnOpt methods are approximately 4.447×10^8 and 3.857×10^8 (same as initially obtained) respectively. The corresponding total number of iterations carried out with the different seed numbers are shown in Fig. 9(b). The average number of iterations for the standard EnOpt method is 20 and for the EPF-EnOpt method is 51.

Example 3

To further explore the benefit of the proposed EPF-EnOpt method, we consider a more realistic industrial standard 3D oil reservoir model (the Reek field designed by Equinor). The associated N_u-dimensional constrained optimization problem of water flooding associated with the Reek field is given by Eqs. (58)–(59). The reservoir model is synthetic with three-phase flow (including oil, water and gas). It is defined on an irregular grid system of dimension $40 \times 64 \times 14$. There are total of 35840 grid cells with distinct sizes. The model is divided into UpperReek, MidReek, and LowerReek zones with six faults and varying porosity and permeability. The model has five production and three injection wells as shown in Fig. 10. Two of the injectors are positioned in the water saturated zones, while the five producers and one injector are spatially distributed throughout the oil containing region based on engineering intuition. Fluid properties are similar to that of light oil. On average, it has approximately 15% porosity with heterogeneous permeability map. The original oil in place (OOIP) is 4.831×10^7 sm^3. The initial average oil, water, and gas saturations are $0.1658, 0.8342$, and 0 respectively. The viscosity (in cP) for saturated oil at varying bubble point pressure is in the interval $[0.09, 1]$ and viscosity of water is 0.01 cP. The densities of oil and water are respectively 732 kg/m^3 and 1000 kg/m^3.

In this example, the injection well is controlled by water injection rate at each control time step. The lower and upper bounds for water injection rate are set to 0 sm^3/day and 10000 sm^3/day respectively. Each production well is controlled by reservoir fluid production rate with a lower limit of 0 sm^3/day and upper limit of 5000 sm^3/day. Bottom hole pressure (BHP) limits are imposed on the wells, specifically maximum 500 bar for the injector and minimum 200 bar for each

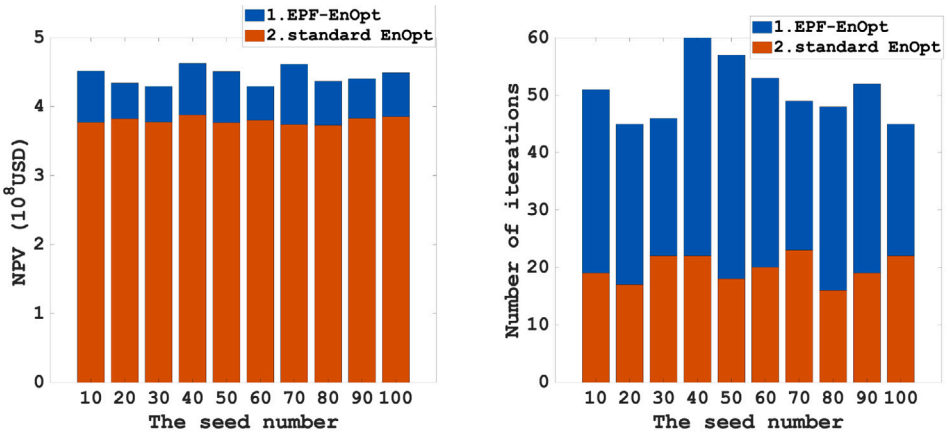

(a) NPV variation with random seed (b) Number of iteration variation with random seed

Fig. 9. (a) Comparison of the change in NPV from the standard EnOpt and EPF-EnOpt methods with random seed. (b) Comparison of the total number of iteration from the standard EnOpt and EPF-EnOpt methods with random seed.

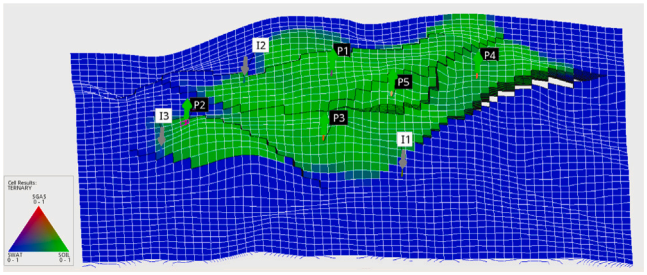

Fig. 10. The initial saturation map for oil, water and gas of the Reek field.

producer. The simulation period for the reservoir is 1110 days and the control time step is set to 30 days. The optimization unknown control vector $\mathbf{u}$ has a total of $(5+3)\times 50 = 296$ components (control variables). Thus, the constrained waterflooding optimization problem is to find the optimal control vector, $\mathbf{u} = \{u_i\}_{i=1}^{296}$ that maximizes the NPV in Eq. (58) subject to the constraints in Eq. (59). Here, the NPV is optimized using the economic parameters listed in Table 2. First, we seek a solution to the optimization problem by using the standard EnOpt approach coupled with the linear transformation (with truncation). In this case, we utilize feasible initial guess, $\mathbf{u}_1$ of control vector (denoted by the "ref control" in Fig. 11) provided by Equinor. The values of other optimization parameters considered in the EnOpt algorithm are given in Table 1.

In 55 iterations, the standard EnOpt algorithm is seen to converge (when $|J(\mathbf{u}_{l+1}) - J(\mathbf{u}_l)| \leq \epsilon_3 |J(\mathbf{u}_l)|$ is sufficiently satisfied) to a suboptimal solution (represented by the "standard EnOpt" in Fig. 11) of the problem (58)–(59). The maximum NPV reached is 4.285×10^9 (in USD) (see the "standard EnOpt" in Fig. 12(a)). Similar to Example 2, we used the proposed EPF-EnOpt method (in Algorithm 2) to solve the subproblems (61) associated with the Reek field waterflooding problem for comparison with the standard EnOpt. We set the initial penalty parameter, r_1 and the growth constant, c to 10 and 1.2 respectively, and $\epsilon_1 = 1.0\times 10^{-5}$ and $\epsilon_2 = 1.0\times 10^{-6}$. The initial guess of solution is taken as $\mathbf{u}(r_1) := \mathbf{u}_1$ (see the "Ref control" in Fig. 11). The same values of parameters in Table 1 are utilized for the unconstrained minimization procedures. Other parameters or transformations not mentioned are the same as before in Example 2. By applying Algorithm 2, the resulting limit of the solutions of subproblems P_k, $k = 1, 2, 3, \ldots, 58$ (equivalently the solution of problem (58)–(59)) is denoted by the "EPF-EnOpt" in Fig. 11. The corresponding value of the objective function (58) at the solution of subproblem, $P_k, k = 1, 2, \ldots, 58$ is represented by the "EPF-EnOpt" in Fig. 12(a). Here, the Algorithm 2 converges to a better suboptimal solution of problem (58)–(59) at the 59th subproblem with a total of 116 unconstrained optimization iterations as shown in Fig. 13. The maximum NPV obtained is 4.556×10^9 (in USD). Therefore, the EPF-EnOpt method yields an increase of 6.324% in NPV over the standard EnOpt approach.

To further illustrate the efficiency and accuracy of the EPF-EnOpt method, we utilized the classical Lagrange function (LGF) method to handle constraints coupled with the standard EnOpt, to solve the optimization problem and compare results with the EPF-EnOpt. The Lagrange function associated with the constrained water flooding optimization problem of the Reek field (using Eqs. (58)–(59)) is given by :

$$L(\mathbf{u}, \boldsymbol{\lambda}^k, r_k) = f(\mathbf{u}) + r_k\Big(\sum_{i=1}^{N_u}\sum_{j=1}^{2}\Big[(\min\{\frac{\lambda_{j,i}}{2r_k} + g_j(u_i), 0\})^2 - (\frac{\lambda_{j,i}}{2r_k})^2\Big]\Big), \quad (62)$$

where $\boldsymbol{\lambda}^k := [\{\lambda_{j,i}^k\}_{i=1}^{N_u}], \forall i = 1, 2$ is the Lagrangian multiplier for the $2N_u$ constraint functions and r_k is the penalty parameter. For each kth subproblem, we estimate the Lagrangian multiplier using:

$$\boldsymbol{\lambda}^{k+1} := \min\{\boldsymbol{\lambda}^k + 2r_k\mathbf{g}(\mathbf{u}), 0\}, \quad \mathbf{g} = [g_1, g_2], \quad (63)$$

and the penalty parameter r_k is updated using Eq. (17). Using the same optimization parameters, initialization, and convergence tolerance as in the EPF-EnOpt method and initial multiplier components, $\lambda_{j,i} = 0$, we sequentially solve (using the standard EnOpt) for the optimal solution of the Lagrangian in Eq. (62). After 66 subproblems, the Lagrangian converges to a suboptimal value as depicted by "LGF-EnOpt" in Fig. 12(a) with a total of 113 unconstrained iterations as shown by "LGF-EnOpt" in Fig. 13. The limit of solutions of the subproblems is shown by "LGF-EnOpt" in Fig. 11 (equivalently a suboptimal solution to the original constrained optimization problem). The maximum NPV obtained is 4.400×10^9 (in USD) which is less than that of the EPF-EnOpt method by 3.55%. The need for the LGF-EnOpt to estimate the Lagrange multiplier in addition to the penalty parameter shows that the method requires more subproblem iterations.

Fig. 12(b) compares the field oil production total from developing the Reek field with the solutions (or control strategies) of the EPF-EnOpt, LGF-EnOpt, standard EnOpt methods respectively, and the reference control. The total field oil production by the EPF-EnOpt, LGF-EnOpt, and standard EnOpt solutions are 1.091×10^6 sm^3, 1.054×10^6sm^6, and 1.037×10^6 sm^3 respectively. The EPF-EnOpt solution gives an increase of approximately 5.207% and 3.510% in oil production over the standard EnOpt and LGF-EnOpt solutions respectively. Also, we compare the corresponding field water production from the three solutions in Fig. 12(c). The total field water production from the EPF-EnOpt, standard EnOpt, and LGF-EnOpt solutions are 3.338×10^6 sm^3, $3.949 \times$

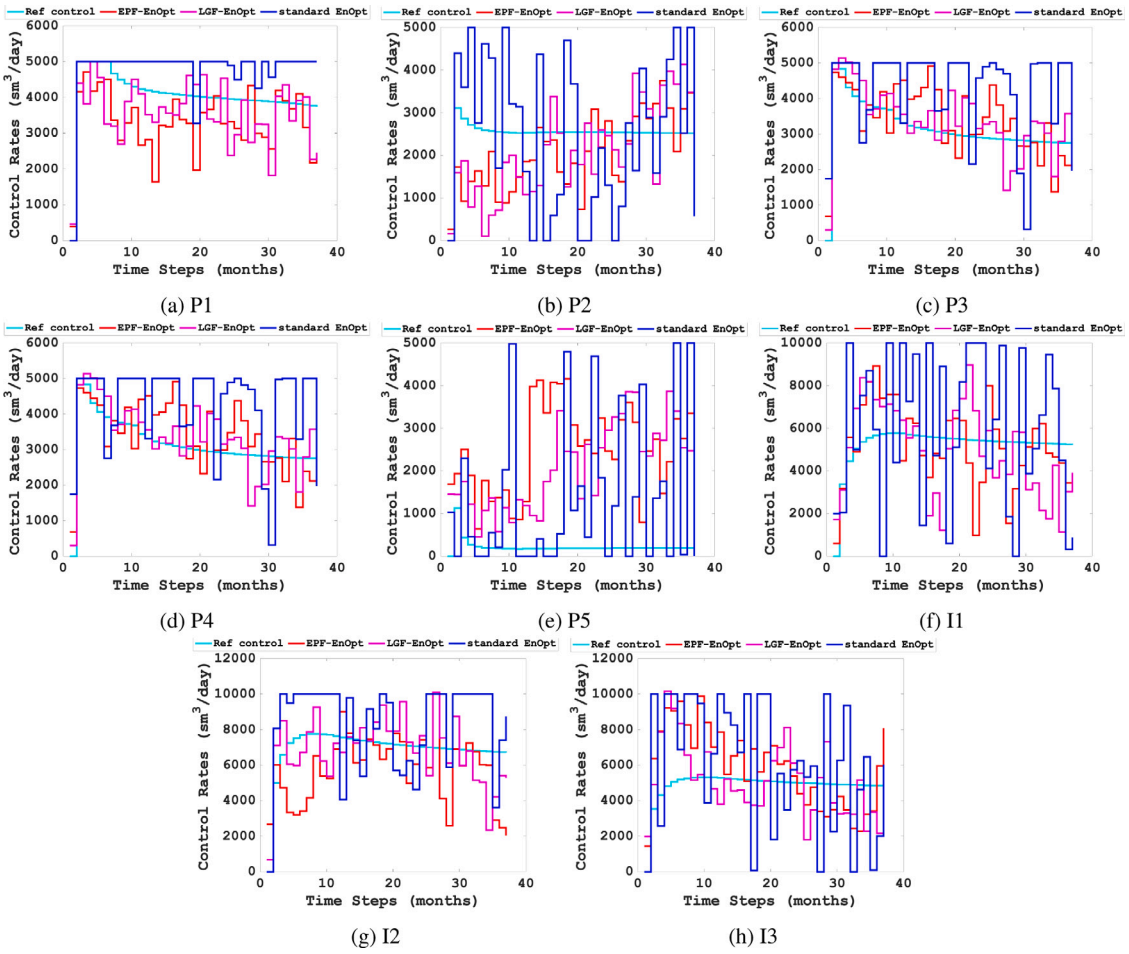

Fig. 11. Comparison of the initial (ref) and optimal solutions from standard EnOpt, EPF-EnOpt, and LGF-EnOpt methods for the constrained optimization problem (58)–(59) associated with the Reek field. Plots (a) to (e) represent the control (production rate) variation profiles at the five producing wells and (f) to (h) denote the control (injection rate) variation profile at the three injection wells.

10^6 sm^3, and 3.152×10^6 sm^3 respectively. It is approximately 15.47% and 20.18% in water production by the EPF-EnOpt and LGF-EnOpt solutions less than the standard EnOpt method. Hence, the EPF-EnOpt has the potential to find a better optimal solution that will not only increase oil production but also reduced field water production. This is similar to the solution obtained by using the LGF-method in Zhang et al. (2016).

6. Conclusion

In this study, a new optimal solution strategy, the EPF-EnOpt method, for non-linear constrained optimization problems (such as the one of hydrocarbon field management) is formulated. The strategy leans on the exterior penalty function method and adaptive EnOpt scheme (with backtracking technique). Because of the inappropriate gradient computation arising from using the traditional truncation of control variables to honor of the underlying constraints, we utilized the exterior PF method to transform the constrained optimization problem to a sequence of unconstrained subproblems. We used the adaptive EnOpt method to sequentially solve the subproblems, which eventually leads to the desired solution of the original constrained optimization problem.

Further, the proposed method is formulated in such a way that mixed (involving equality and inequality) constraint problems can be solved efficiently and robustly and also its performance (in terms of convergence rate and accuracy) is compared with the standard EnOpt method. The optimization results of the analytical 2D constrained Rosenbrock problem (see Example 1) showed that the EPF-EnOpt method has a faster convergence rate (and hence more efficient). The solutions of the practical N_u- dimensional constrained water flooding optimization problem associated with the 2D 5Spot field (see Example 2) and 3D Reek field (see Example 3) showed that the method is more accurate than the standard EnOpt approach. In addition to increasing oil production, the EPF-EnOpt methods can provide a solution with less impact (in terms of water production) on the environment compared to the standard EnOpt with traditional constraint handling techniques (as shown in Fig. 12(c)). For the Reek field we also compared the EPF-EnOpt method with the classical Lagrangian constraint handling technique. The results showed higher NPV was obtained with the EPF-EnOpt.

It is noted that the minima of subproblems obtained lie within the feasible region of interest because of our choice of parametric values (irrespective of using infeasible (see Example 1) or feasible (see Example 2) solution initialization). However, this is not always true as different sets of values of parameters such as penalty parameter, growth constant, optimization parameters (such as the number of perturbation and initial step size, and backtracking constants) can change trend of solutions. Also, the size of subproblems and number of optimization iterations before convergence is found to significantly rely on the values assigned to these parameters. Therefore, careful selection of parametric values is the key if strictly feasible solutions are required and for fast convergence rate.

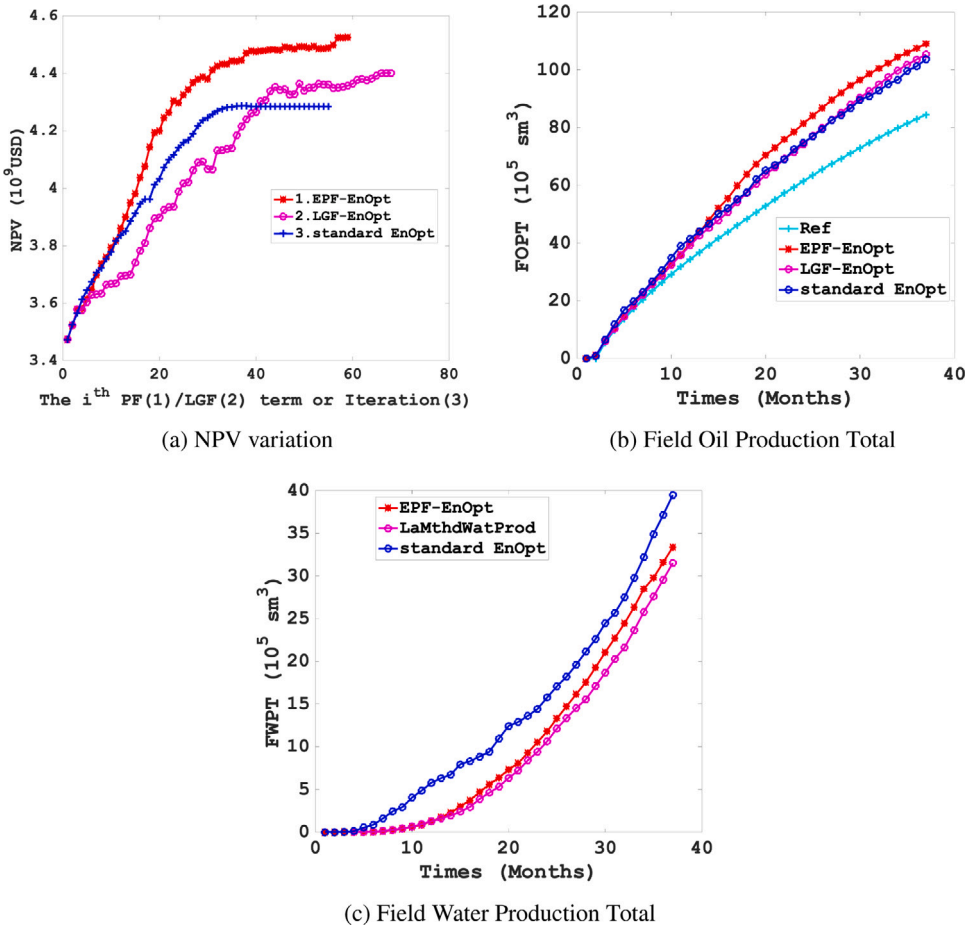

(a) NPV variation

(b) Field Oil Production Total

(c) Field Water Production Total

Fig. 12. (a) Comparison of the change in NPV with iteration (for standard EnOpt) or penalty term or Lagrang e function (or subproblem). (b) Comparison of the field oil production total (FOPT) from reference(Ref), standard EnOpt, and EPF-EnOpt controls.(c) Comparison of the field water production total (FWPT) from standard EnOpt and EPF-EnOpt controls.

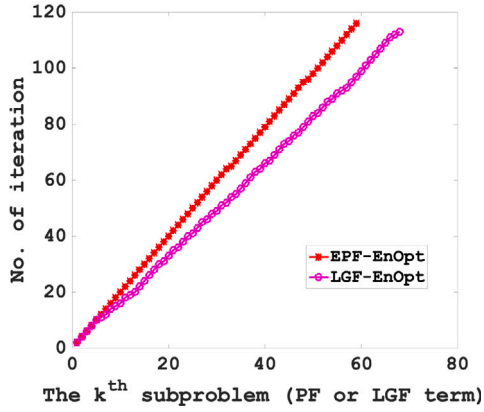

Fig. 13. Plot of cumulative number of unconstrained minimization iteration versus the *kth* subproblem for the Reek field problem.

For future reference, the present methodology will be used to solve robust constrained optimization problems of oil reservoirs with uncertain geological parameters. In this paper, we considered bound constraint optimization problems. However, solution of optimization problem with mixed or more complex linear or non-linear constraints are possible. Also, there is room to carry out sensitivity analysis with influential parameters on the EPF-EnOpt method.

CRediT authorship contribution statement

Micheal B. Oguntola: Carried out the mathematical formulations and computations of the study, Analyzed the data, Wrote the paper, Contributed to manuscript revisions. **Rolf J. Lorentzen:** Conceived and supervised the study, Contributed to manuscript revisions.

Declaration of competing interest

The authors declare that they have no known competing financial interests or personal relationships that could have appeared to influence the work reported in this paper.

Acknowledgments

The authors would like to thank Equinor ASA for developing and sharing the Reek field data. Further, the authors acknowledge the Research Council of Norway and the industry partners, ConocoPhillips Skandinavia AS, Aker BP ASA, Vår Energi AS, Equinor Energy ASA, Neptune Energy Norge AS, Lundin Energy Norway AS, Halliburton AS, Schlumberger Norge AS, Wintershall Dea Norge AS, of The National IOR Centre of Norway for the support. All authors approved the final version of the manuscript.

References

Aanonsen, S.I., Nævdal, G., Oliver, D.S., Reynolds, A.C., Vallès, B., et al., 2009. The ensemble Kalman filter in reservoir engineering–a review. Spe J. 14 (03), 393–412.

Amari, S.-I., 1998. Natural gradient works efficiently in learning. Neural Comput. 10 (2), 251–276. http://dx.doi.org/10.1162/089976698300017746.

Arouri, Y., Sayyafzadeh, M., 2020. An accelerated gradient algorithm for well control optimization. J. Pet. Sci. Eng. 190, 106872.
Bagirov, A., Karmitsa, N., Mäkelä, M.M., 2014. Introduction to Nonsmooth Optimization: Theory, Practice and Software. Springer.
Chen, Y., Oliver, D.S., Zhang, D., 2009. Efficient ensemble-based closed-loop production optimization. SPE J. 14 (04), 634–645.
Chen, Y., Oliver, D.S., et al., 2010. Ensemble-based closed-loop optimization applied to brugge field. SPE Reser. Eval. Eng. 13 (01), 56–71.
Chen, G., Zhang, K., Xue, X., Zhang, L., Yao, J., Sun, H., Fan, L., Yang, Y., 2020. Surrogate-assisted evolutionary algorithm with dimensionality reduction method for water flooding production optimization. J. Pet. Sci. Eng. 185, 106633.
Deb, K., 2012. Optimization for Engineering Design: Algorithms and Examples. PHI Learning Pvt. Ltd.
Do, S.T., Reynolds, A.C., 2013. Theoretical connections between optimization algorithms based on an approximate gradient. Comput. Geosci. 17 (6), 959–973.
Epelle, E.I., Gerogiorgis, D.I., 2020. Adjoint-based well placement optimisation for enhanced oil recovery (EOR) under geological uncertainty: From seismic to production. J. Pet. Sci. Eng. 190, 107091.
Fonseca, R.R.-M., Chen, B., Jansen, J.D., Reynolds, A., 2017. A stochastic simplex approximate gradient (StoSAG) for optimization under uncertainty. Internat. J. Numer. Methods Engrg. 109 (13), 1756–1776.
Fonseca, R.M., Kahrobaei, S.S., Van Gastel, L.J.T., Leeuwenburgh, O., Jansen, J.D., 2015. Quantification of the impact of ensemble size on the quality of an ensemble gradient using principles of hypothesis testing. In: SPE Reservoir Simulation Symposium. Society of Petroleum Engineers.
Fonseca, R., Leeuwenburgh, O., Van den Hof, P., Jansen, J.-D., et al., 2014. Improving the ensemble-optimization method through covariance-matrix adaptation. SPE J. 20 (01), 155–168.
Foroud, T., Baradaran, A., Seifi, A., 2018. A comparative evaluation of global search algorithms in black box optimization of oil production: A case study on Brugge field. J. Pet. Sci. Eng. 167, 131–151.
Han, S.-P., Mangasarian, O.L., 1979. Exact penalty functions in nonlinear programming. Math. Program. 17 (1), 251–269.
Hock, W., Schittkowski, K., 1981. Test Examples for Nonlinear Codes. Springer-Verlag.
Hutahaean, J., Demyanov, V., Christie, M., 2019. Reservoir development optimization under uncertainty for infill well placement in brownfield redevelopment. J. Pet. Sci. Eng. 175, 444–464.
Islam, J., Vasant, P.M., Negash, B.M., Laruccia, M.B., Myint, M., Watada, J., 2020. A holistic review on artificial intelligence techniques for well placement optimization problem. Adv. Eng. Softw. 141, 102767.
Jansen, J., 2011. Adjoint-based optimization of multi-phase flow through porous media - A review. In: 10th ICFD Conference Series on Numerical Methods for Fluid Dynamics (ICFD 2010). Comput. & Fluids 46 (1), 40–51. http://dx.doi.org/10.1016/j.compfluid.2010.09.039.
Jansen, J.-D., Brouwer, R., Douma, S.G., 2009. Closed loop reservoir management. In: SPE Reservoir Simulation Symposium. Society of Petroleum Engineers.
Jesmani, M., Jafarpour, B., Bellout, M.C., Foss, B., 2020. A reduced random sampling strategy for fast robust well placement optimization. J. Pet. Sci. Eng. 184, 106414.
Jung, S., Lee, K., Park, C., Choe, J., 2018. Ensemble-based data assimilation in reservoir characterization: A review. Energies 11 (2), 445.
Li, G., Reynolds, A.C., 2011. Uncertainty quantification of reservoir performance predictions using a stochastic optimization algorithm. Comput. Geosci. 15 (3), 451–462.
Liu, Z., Reynolds, A.C., et al., 2019. An SQP-filter algorithm with an improved stochastic gradient for robust life-cycle optimization problems with nonlinear constraints. In: SPE Reservoir Simulation Conference. Society of Petroleum Engineers.
Lorentzen, R.J., Berg, A., Nævdal, G., Vefring, E.H., 2006. A new approach for dynamic optimization of water flooding problems. In: Intelligent Energy Conference and Exhibition. Society of Petroleum Engineers.
Lu, R., Forouzanfar, F., Reynolds, A.C., et al., 2017. Bi-objective optimization of well placement and controls using stosag. In: SPE Reservoir Simulation Conference. Society of Petroleum Engineers.
Mirzaei-Paiaman, A., Santos, S.M., Schiozer, D.J., 2021. A review on closed-loop field development and management. J. Pet. Sci. Eng. 108457.
Nocedal, J., Wright, S.J., 2006. Numerical Optimization, second ed. Springer.
Oguntola, M., Lorentzen, R., 2020. On the robust value quantification of polymer EOR injection strategies for better decision making. In: ECMOR XVII, 2020. European Association of Geoscientists & Engineers, pp. 1–25.
Ramaswamy, K.R., Fonseca, R.M., Leeuwenburgh, O., Siraj, M.M., Van den Hof, P.M.J., 2020. Improved sampling strategies for ensemble-based optimization. Comput. Geosci. 24 (3), 1057–1069.
Rao, S.S., 2019. Engineering Optimization: Theory and Practice. John Wiley & Sons.
Sarma, P., Aziz, K., Durlofsky, L.J., 2005. Implementation of adjoint solution for optimal control of smart wells. In: SPE Reservoir Simulation Symposium. Society of Petroleum Engineers.
Sarma, P., Chen, W.H., Durlofsky, L.J., Aziz, K., 2006. Production optimization with adjoint models under nonlinear control-state path inequality constraints. In: Intelligent Energy Conference and Exhibition. Society of Petroleum Engineers.
Sarma, P., Chen, W.H., et al., 2008. Efficient well placement optimization with gradient-based algorithms and adjoint models. In: Intelligent Energy Conference and Exhibition. Society of Petroleum Engineers.
Semnani, A., Ostadhassan, M., Xu, Y., Sharifi, M., Liu, B., 2021. Joint optimization of constrained well placement and control parameters using teaching-learning based optimization and an inter-distance algorithm. J. Pet. Sci. Eng. 203, 108652.
Snyman, J.A., Wilke, D.N., 2018. Practical Mathematical Optimization: Basic Optimization Theory and Gradient-Based Algorithms, vol. 133. Springer.
Spall, J.C., 1998. Implementation of the simultaneous perturbation algorithm for stochastic optimization. IEEE Trans. Aerosp. Electron. Syst. 34 (3), 817–823.
Spall, J.C., Hill, S.D., Stark, D.R., 2006. Theoretical framework for comparing several stochastic optimization approaches. In: Probabilistic and Randomized Methods for Design under Uncertainty. Springer, pp. 99–117.
Stordal, A.S., Szklarz, S.P., Leeuwenburgh, O., 2016. A theoretical look at ensemble-based optimization in reservoir management. Math. Geosci. 48 (4), 399–417.
Sun, Y., Liu, Z., Dong, X., 2019. Rate optimization of fractional flow reservoir model based on the continuous adjoint method. J. Pet. Sci. Eng. 183, 106346.
Sun, W., Yuan, Y.-X., 2006. Optimization Theory and Methods: Nonlinear Programming, vol. 1. Springer Science & Business Media.
Xu, L., Zhao, H., Li, Y., Cao, L., Xie, X., Zhang, X., Li, Y., 2018. Production optimization of polymer flooding using improved Monte Carlo gradient approximation algorithm with constraints. J. Circuits Syst. Comput. 27 (11), 1850167.
Yan, X., Reynolds, A.C., 2014. Optimization algorithms based on combining FD approximations and stochastic gradients compared with methods based only on a stochastic gradient. SPE J. 19 (05), 873–890.
Zandvliet, M., Handels, M., van Essen, G., Brouwer, R., Jansen, J.-D., 2008. Adjoint-based well-placement optimization under production constraints. Spe J. 13 (04), 392–399.
Zhang, L., Cui, C., Ma, X., Sun, Z., Liu, F., Zhang, K., 2019. A fractal discrete fracture network model for history matching of naturally fractured reservoirs. Fractals 27 (01), 1940008.
Zhang, Y.T., Lorentzen, R.J., Stordal, A.S., 2018a. Practical use of the ensemble-based conjugate gradient method for production optimization in the brugge benchmark study. In: SPE Norway One Day Seminar. Society of Petroleum Engineers.
Zhang, Y.T., Stordal, A.S., Lorentzen, R.J., Chang, Y., 2018b. A novel ensemble-based conjugate gradient method for reservoir management. In: SPE Norway One Day Seminar. Society of Petroleum Engineers.
Zhang, K., Zhang, X., Ni, W., Zhang, L., Yao, J., Li, L., Yan, X., 2016. Nonlinear constrained production optimization based on augmented Lagrangian function and stochastic gradient. J. Pet. Sci. Eng. 146, 418–431.
Zhao, H., Chen, C., Do, S., Oliveira, D., Li, G., Reynolds, A., et al., 2013. Maximization of a dynamic quadratic interpolation model for production optimization. SPE J. 18 (06), 1–012.
Zhao, X., Zhang, K., Chen, G., Xue, X., Yao, C., Wang, J., Yang, Y., Zhao, H., Yao, J., 2020. Surrogate-assisted differential evolution for production optimization with nonlinear state constraints. J. Pet. Sci. Eng. 194, 107441.
Zhou, K., Hou, J., Zhang, X., Du, Q., Kang, X., Jiang, S., 2013. Optimal control of polymer flooding based on simultaneous perturbation stochastic approximation method guided by finite difference gradient. Comput. Chem. Eng. 55, 40–49.